FAST NUMERICAL PRICING OF BARRIER OPTIONS UNDER STOCHASTIC VOLATILITY AND JUMPS

FAST NUMERICAL PRICING OF BARRIER OPTIONS UNDER STOCHASTIC VOLATILITY AND JUMPS*

C. GUARDASONI† AND S. SANFELICI ‡

Abstract. In this paper, we prove the existence of an integral closed-form solution for pricing barrier options in both Heston and Bates frameworks. The option value depends on time, on the price and on the volatility of the underlying asset and it can be computed as the solution of a two dimensional pricing partial integro-differential equation. The integral representation formula of the solution is derived by projection of the differential equation and exploiting the properties of the adjoint operator. We derive the expression of the fundamental solution (Green's function) necessary for the integral representation formula. The computation is based on the interpretation of the fundamental solution as the joint transition probability density function of the underlying asset price and variance and is obtained through Fourier inverse transform of a suitable conditional characteristic function. We propose a numerical scheme to approximate the option price based on the classical Boundary Element Method and we provide two numerical examples showing the computational efficiency and accuracy of the proposed new method. The algorithm can be modified to compute greeks as well.

Key words. Boundary Element Method, Barrier options, Bates model, Heston model.

AMS subject classifications. 65M38, 91G60, 91G20, 65M80.

1. Introduction. Option pricing is an important field of research in financial economics from both a theoretical and practical point of view. The pioneering work of Black and Scholes ([7]) laid the foundations of the field and stimulated important research in option pricing theory and its mathematical models. However, it is well known that the description of financial market behavior provided by this model is not satisfactory. Very well known observed empirical statistical features of the log prices, such as heavy tails, volatility clustering, aggregational gaussianity, cannot be correctly described on the basis of the lognormal assumption on which the Black-Scholes model stands. The volatility smile and smirk are other relevant phenomena that cannot be explained on the basis of a Black-Scholes description. A huge effort has been made in the last few years in order to overcome the intrinsic limitations of the Black-Scholes model for financial derivatives. Several different extensions have been introduced in order to give a more satisfactory description of financial markets, but the main contributions in this direction can be grouped in two different classes of models, the so called *stochastic volatility models* and the *models with jumps*. An extended literature is available on both kind of approaches, giving a more realistic description of the price evolution in financial markets where both features of stochastic volatility and jumps can be present. This has naturally led to the introduction of more realistic but more complicated models, for which no closed-form pricing formulas are available. In particular, the *Bates model* ([5]) combines a Merton jump-diffusion model ([24]) with a stochastic volatility model of the Heston type ([22]).

From a different perspective, modern derivative contracts depart from the classical European paradigm of plain vanilla options and require the use of sophisticated numerical methods to be priced. In particular, in recent years *barrier options* have become increasingly popular and frequently traded financial instruments. Barrier op-

*This work was supported by the Italian "National Group of Computing Science (GNCS-INdAM)".

†Department of Mathematics, University of Parma (chiara.guardasoni@unipr.it).

‡Department of Economics, University of Parma (simona.sanfelici@unipr.it).

tions are path-dependent exotic options that become activated or null if the underlying asset reaches certain levels. There are four main types of barrier options that can either have call or put feature: down-and-in, down-and-out, up-and-in and up-and-out. The "down" and "up" terms refer to the position of the barrier relative to the initial underlying price. The "in" and "out" terms specify the type of the barrier, referring to activating and nullifying when the barrier is breached respectively. A down-and-out call option for instance becomes nullified if the price of the underlying falls below the barrier. Despite being frequently traded nowadays, barrier options are still known as exotic options since they cannot be replicated by a finite combination of standard products, i.e. vanilla call and put options, future contracts etc., and a closed-form pricing formula is not available unless we assume a Black-Scholes framework for the underlying.

For these more advanced financial models, pricing is traditionally based on Monte Carlo methods that, anyway, are affected by high computational costs and inaccuracy due to their intrinsic slow convergence.

Other possible approaches to barrier option pricing are offered by Finite Difference Finite Element and Finite Volume methods [27], [1] or Binomial and Trinomial Trees [8], [28], [30]. Lattice methods are actually explicit finite difference schemes in which the time-step is tied to the spatial grid-size in order to guarantee numerical stability. Therefore, they are not very efficient for pricing barrier options because they require a fine grid spacing to handle barrier conditions and hence a very large number of time-steps.

In the present paper, we propose a semi-analytical pricing method for this special class of path-dependent options under the Bates framework, based on the Boundary Element Method (BEM). Since 1970s, with the introduction of the electronic computers, Boundary Element Method (BEM) has been largely used for approximating solutions to partial differential equations (PDEs) in Physics and Engineering ([12]) and in particular, more recently, its application has been refined for time-dependent problems that involve more difficult theoretical analysis (cfr. [14] for a deep survey and references on this topic). Despite this, only very few and very recent contributes ([2],[3],[4]) are available in literature about its application to Quantitative Finance and, more in general, to Economics ([23]).

The advantages of BEM, when compared to domain methods, such as Finite Element Methods (FEM) or Finite Difference Methods (FDM), are well known ([11]): only the boundary of the domain needs to be discretized and, in particular, exterior problems with unbounded domains but bounded boundaries are handled as easily as interior problems. Therefore, this feature makes this method quite interesting when considering options with barriers: the solution in the interior of the domain is approximated with a rather high convergence rate and can be evaluated at particular points of the domain and not necessarily everywhere on a defined grid; far field boundary conditions are implicitly satisfied.

BEM is based on the representation of the solution of the differential problem in terms of integral equations. For plain vanilla options, this integral formulation reduces to the fundamental evaluation formula for option pricing, i.e. the computation of the option price as discounted expectation of the final payoff under suitable probability measure. For barrier options, the integral representation formula and the boundary condition at the barrier allow to obtain an equation that can be solved by integration in time and variance only. Therefore, the dimensionality of the problem is reduced by one. The integration domain is bounded in time and unbounded in variance. However,

exploiting the far-field properties of the option price and of the kernels appearing in the integrals, it can be truncated to compute the integrals numerically. Alternatively, one can use an infinite element approach on the unbounded domain as in [31].

One of the main difficulties that could arise applying this method, concerns the necessary explicit knowledge of a *fundamental solution* for the differential equation governing the price of the contingent claim, namely the *conditional* (i.e. *transition*) *probability density function* (PDF), that is generally available only for linear partial differential equations with constant or some specific variable coefficients. The fundamental solution is available in Black-Scholes case but, when considering more complicated models such as Heston ([22]) or Bates ([5]), it may be available only through Fourier inverse transform. In particular, when pricing exotic options, the joint transition probability density function of stock log-price and variance must be computed.

For Black-Scholes equation, BEM is really efficient and accurate as already deeply investigated in [4] and [21], where the authors have tested the method for different types of barrier options. Here, we will show that this method maintains these qualities also for more general and possibly multifactor models like Heston's and Bates', when we don't know explicitly the analytical expression for the fundamental solution. BEM consists of two phases: first, the numerical computation of a service functional on the boundary, then the *post-processing* necessary to get the solution of the starting differential problem. In particular, a great advantage of the BEM over Finite Difference approaches is that, in the post-processing, only one evaluation is needed for one spot price and variance level. Moreover, differently from Monte Carlo methods, if the option is to be priced for a new asset value one can implement only the post-processing with a great computational saving. This makes sensitivity analysis easily workable numerically. In the post-processing phase, closed-form formulas for the most important greeks can be easily derived as well.

The paper is organized as follows: in §2, the Bates jump-diffusion stochastic volatility model is presented. After recalling the main issues concerning the option pricing under Bates' framework, we provide an integral representation formula which allows to price barrier options starting from a computation of the joint transition probability density function of stock log-price and variance; we derive the expression of the density function necessary for the integral representation formula. Moreover, we provide a closed-form formula to compute the option delta. In §3, we discuss how to numerically solve the boundary integral problem by the BEM approach combined with Fourier inverse transform and discuss technical details of implementation. In §4, we perform simulations on call options with a single barrier under both Heston and Bates models to show the accuracy and the computational savings obtained with BEM; the efficiency of our proposed approach is compared to the performance of the Monte Carlo method. Section 5 concludes. Technical details of the proofs are postponed to the Appendix.

2. Boundary integral formulation of a barrier option value under Bates model. Bates model [5] provides an extension of the Heston stochastic volatility model by considering jumps in the stock price process

$$\begin{aligned} dx_t &= \left(\mu - \delta - \tfrac{1}{2}v_t\right)dt + \sqrt{v_t}dW_t^1 + j_N(t)dN(t) \\ dv_t &= -\lambda(v_t - \bar{v})dt + \eta\sqrt{v_t}dW_t^2, \end{aligned} \tag{2.1}$$

where v_t is the variance process i.e. the square of volatility and $x_t = \log S_t$ is the logarithm of the underlying asset value S_t; W_t^1, W_t^2 are correlated Brownian motions

with instantaneous correlation ρ, μ is the drift, δ the dividend yield. Here $N(t)$ is a Poisson process with intensity ξ and $j_N(t)$ are normally distributed jump sizes in the logarithmic price, with expectation μ_j and variance σ_j^2. The Poisson process $N(t)$ is independent of the Brownian motions and the jump sizes. The stochastic differential equation (SDE) for the variance can be recognized as a mean-reverting square root process, as originally proposed by [15] to model the spot interest rate. λ is the speed of mean reversion, $\bar{v}$ is the mean level of variance and η is the volatility of volatility. The Feller condition, $2\lambda\bar{v} \geq \eta^2$, guarantees that v_t stays positive; otherwise, it may reach zero.

Under the martingale measure $\mathbb{Q}$, the drift is given by $r-\xi\bar{k}$, where $\bar{k} = \mathbb{E}[e^{j_N(t)}-1] = \exp\left(\mu_j + \frac{\sigma_j^2}{2}\right) - 1$ and r is the risk-free interest rate. Under $\mathbb{Q}$, the characteristic function of the log-price process in the Bates model can be obtained by multiplying the characteristic function $\phi_T^c(\omega; x_0, v_0, t_0)$ of the continuous component x_t^c of x_t in the Heston model by the characteristic function of the jumps which in this case is (see e.g. [13])

$$\phi_T^J(\omega; t_0) = \exp\{(T-t_0)\xi(e^{-\sigma_j^2\omega^2/2+\mathbf{i}\mu_j\omega} - 1)\}. \tag{2.2}$$

Therefore,

$$\phi_T(\omega; x_0, v_0, t_0) = \mathbb{E}[e^{\mathbf{i}\omega x_T}|x_{t_0} = x_0, v_{t_0} = v_0] = \phi_T^c(\omega; x_0, v_0, t_0) \cdot \phi_T^J(\omega; t_0), \tag{2.3}$$

where

$$\phi_T^c(\omega; x_0, v_0, t_0) = \mathbb{E}[e^{\mathbf{i}\omega x_T^c}|x_{t_0} = x_0, v_{t_0} = v_0] =$$
$$= \exp\left\{\mathbf{i}\omega(r-\bar{k}\xi-\delta)(T-t_0) + \frac{v_0}{\eta^2}\left(\frac{1-e^{-D(T-t_0)}}{1-Ce^{-D(T-t_0)}}\right)(\lambda-\rho\eta\mathbf{i}\omega-D)+\right.$$
$$\left.+\frac{\lambda\bar{v}}{\eta^2}\left((T-t_0)(\lambda-\rho\eta\mathbf{i}\omega-D) - 2\log\left(\frac{1-Ce^{-D(T-t_0)}}{1-C}\right)\right) + \mathbf{i}\omega x_0\right\},$$

where $D = \sqrt{(\lambda-\rho\eta\mathbf{i}\omega)^2 + (\omega^2+\mathbf{i}\omega)\eta^2}$ and $C = \frac{\lambda-\rho\eta\mathbf{i}\omega-D}{\lambda-\rho\eta\mathbf{i}\omega+D}$.

Model (2.1) allows for an analytically tractable method of pricing European options, which are priced as discounted expected value of their terminal payoffs under the risk neutral probability measure [5]. The two dimensional pricing partial differential equation (PDE) for a contingent claim in the Bates model can be deduced from hedging arguments. In case of a one-dimensional model such as the Black-Scholes framework, a self-financing portfolio is constructed via an option and $-\Delta$ units of stocks. Whereas for Bates' two dimensional model, the risk associated with the random volatility needs to be hedged as well. Using Itô's lemma and arbitrage arguments, the following two dimensional pricing partial integro-differential equation (PIDE) is derived ([5])

$$\frac{\partial V}{\partial t} + \frac{1}{2}v\frac{\partial^2 V}{\partial x^2} + \rho\eta v\frac{\partial^2 V}{\partial x\partial v} + \frac{1}{2}\eta^2 v\frac{\partial^2 V}{\partial v^2} + \left(r-\xi\bar{k}-\delta-\frac{1}{2}v\right)\frac{\partial V}{\partial x} - (\lambda(v-\bar{v})-\theta v)\frac{\partial V}{\partial v}$$
$$-rV + \int_{-\infty}^{+\infty}[V(x+z,v,t)-V(x,v,t)]\xi\frac{1}{\sqrt{2\pi}\sigma_j}\exp\left(-\frac{(z-\mu_j)^2}{2\sigma_j^2}\right)dz = 0, \tag{2.4}$$

with the final condition

$$V(x,v,T) = g(x),$$

where $V = V(x, v, t)$ is the price of the contingent claim, g is the payoff of the contract at expiry and θ is known as the market price of volatility risk. The market price of risk will be handled by the other parameters, because the model is usually calibrated to the market. So, θ can be chosen to equal zero, i.e. factor risk premia have been internalized in the stochastic structure.
The analytical solution of the partial integro-differential problem for a European plain vanilla option can be expressed in terms of the moment generating functions or equivalently of the characteristic functions associated to suitable "stock-adjusted" and "money market-adjusted" probabilities.
In the case of more complex exotic options such as barrier options, closed-form solutions are no longer available and we have to resort to numerical approximation. Monte Carlo Methods are inherently inexact and affected by slow convergence. On the other hand, using Finite Element Methods (FEM) or Finite Difference Methods (FD) entails the need to define suitable final and boundary conditions based on analytic or financial considerations. Often, these conditions hold only approximately or, if exact, they have to be numerically approximated. This entails a tradeoff between accuracy and computational cost by considering suitably large computational domains such that possible errors occurring at the boundary do not affect the option value in the region of interest. The issue of defining suitable boundary or far-field conditions for a barrier option has been faced among others by [25], [31].
The BEM approach avoids these shortcomings of more traditional numerical approaches, as it poses the solution to the PDE (2.4) in an integral form that implicitly satisfies the limiting boundary conditions as soon as we know its fundamental solution G, namely the transition probability density function of the underlying asset x. Consider a down-and-out call option i.e. an exotic option that is extinguished when the price $S_t = \exp(x_t)$ of the underlying asset goes down enough to breach an assigned lower barrier L. Obviously, we have

$$u(x, v, t) = 0 \qquad \text{for} \quad x \in (-\infty, L]\,,\ v \in \Omega_v = (0, +\infty)\,,\ t \in [0, T]\,. \tag{2.5}$$

Moreover, in this case $g(x) = (e^x - E)^+ = \max(e^x - E, 0)$. The following *integral representation formula* holds

THEOREM 2.1. *The undiscounted price $u(x, v, t) = V(x, v, t)e^{r(T-t)}$ of a down-and-out call option can be expressed for $x \in \Omega_x = [\log(L), +\infty)$, $v \in \Omega_v = (0, +\infty)$, $t \in [0, T]$ in the integral form*

$$\begin{aligned} u(x, v, t) = &\int_{\Omega_x}\int_{\Omega_v} (e^y - E)^+ G(y, w, T; x, v, t)\,dw\,dy + \\ &- \int_t^T \int_{\Omega_v} \frac{w}{2} G(\log(L), w, s; x, v, t) \frac{\partial u}{\partial y}(\log(L), w, s)\,dw\,ds\,. \end{aligned} \tag{2.6}$$

Proof. Details of the proof are contained in the Appendix A. □

Note that we can obtain similar integral representation formulas also for options with different single or double barriers (down/up, in/out) just resulting in different boundary conditions for the PIDE[1].
As far as the payoff function depends only on the stock value and not on the variance

[1] In the case of a plain vanilla option, i.e. assuming $L = 0$, taking into account the vanishing boundary conditions for G on the boundary $\partial\Omega$ of the domain $\Omega = (-\infty, +\infty) \times \Omega_v$, we can represent

level, after integration over Ω_v, the fundamental solution needed in the first integral of (2.6) can be recovered from the characteristic function (2.3) for the logarithmic price only, by numerical Fourier inverse transform[2] since

$$\begin{aligned}\widetilde{G}(y,T;x,v,t) &:= \int_{\Omega_v} G(y,w,T;x,v,t)dw = \\ &= \mathcal{F}^{-1}[\phi_T](y,T;x,v,t) = \frac{1}{2\pi}\int_{-\infty}^{+\infty}\phi_T(\omega;x,v,t)e^{-\mathbf{i}\omega y}d\omega.\end{aligned} \tag{2.7}$$

Concerning (2.7), the main difference between Bates' model and univariate models such as Black and Scholes' [21] is that in the former the transition density is not only conditioned on the initial logarithmic stock price, but also on the initial variance. For more complex payoffs, possibly depending on the variance level, as well as in the second integral of (2.6), the required fundamental solution G corresponds to the joint transition probability density function of log-returns and variance

$$G(y,w,s;x,v,t) = p(y,w,s;x,v,t), \quad \text{for } t<s. \tag{2.8}$$

To the best of our knowledge, no closed-form analytical espression is available for this density in the Bates model and in the following we show how to derive it. Technical details of the proofs are postponed to the Appendix.
Let us denote by $p(x_T,v_T,T;x_0,v_0,t_0)$ the transition probability density from x_0 and v_0 at t_0 to x_T and v_T at T, namely the fundamental solution, where x_0, v_0, x_T and v_T represent the logarithm of the initial stock price, the initial variance, the logarithm of the stock price at maturity and the variance at maturity, respectively. In the two-dimensional case, the transition density cannot be written in terms of the changes in the logarithmic stock price and the variance because the Eq.(2.4) has not constant coefficient with respect to the variance, i.e. the identity $p(x_T,v_T,T;x_0,v_0,t_0) = p(x_T-x_0,v_T-v_0,T-t_0)$, does not hold in general. Nevertheless, it can be written in terms of $z_x := x_T - x_0$, $T-t_0$ and v_T, given the initial values at t_0. In particular, we have

LEMMA 2.2. *The transition density of the variance v_T conditioned on v_0 in the CIR model is*

$$p_v(v_T,T-t_0|v_0) = ce^{-b-q}\left(\frac{q}{b}\right)^{\frac{a-1}{2}} I_{a-1}(2\sqrt{bq}),$$

where $c = 2\lambda/((1-e^{-\lambda(T-t_0)})\eta^2)$, $b = cv_0e^{-\lambda(T-t_0)}$, $q = cv_T$, $a = 2\lambda\bar{v}/\eta^2$ and $I_a(q)$ is the modified Bessel function of the first kind.

---

the price as

$$u(x,v,t) = \int_{\Omega_x}\int_{\Omega_v}(e^y - E)^+ G(y,w,T;x,v,t)dwdy,$$

implying that the integral representation formula we are introducing reduces to the traditional Green's function approach.

[2]We define the Fourier transform of a function $f(x)$ as

$$\widehat{f}(\omega) := \mathfrak{F}[f](\omega) = \int_{-\infty}^{\infty} f(x)e^{\mathbf{i}\omega x}dx$$

and the Fourier inverse transform as

$$f(x) := \mathfrak{F}^{-1}[\widehat{f}](x) = \frac{1}{2\pi}\int_{-\infty}^{\infty}\widehat{f}(\omega)e^{-\mathbf{i}\omega x}d\omega\,.$$

Proof. See [17]. □

Moreover, we can prove the following

THEOREM 2.3. *The transition density for Bates model can be computed as*

$$p(x_T, v_T, T; x_0, v_0, t_0) = p_v(v_T, T - t_0|v_0)p(z_x, T - t_0|v_T, v_0), \tag{2.9}$$

The transition density function $p(z_x, T - t_0|v_T, v_0)$ of the logarithm of the stock price given v_0 and given v_T is known through its Fourier transform w.r.t. the variable z_x

$$\begin{aligned}\hat{p}(\omega; v_0, v_T, T - t_0) &= \exp\left\{\mathbf{i}\omega(r - \delta - \bar{k}\xi)(T - t_0) + \frac{\rho}{\eta}(v_T - v_0 - \lambda\bar{v}(T - t_0))\right\} \times \\ &\Phi\left(\omega\left(\frac{\lambda\rho}{\eta} - \frac{1}{2}\right) + \frac{\omega^2}{2}\mathbf{i}(1 - \rho^2)\right) \exp\{(T - t_0)\xi(e^{-\sigma_j^2\omega^2/2 + \mathbf{i}\mu_j\omega} - 1)\},\end{aligned} \tag{2.10}$$

where $\Phi(a)$ is the characteristic function of the integrated variance $\int_{t_0}^{T} v(s)ds$ given v_0 and v_T.

Proof. See the Appendix B. □

In particular, the following result holds

PROPOSITION 2.4. *For $a \in \mathbb{C}$,*

$$\begin{aligned}\Phi(a) &= \frac{\gamma(a)e^{-\frac{1}{2}(\gamma(a)-\lambda)(T-t_0)}(1 - e^{-\lambda(T-t_0)})}{\lambda(1 - e^{-\gamma(a)(T-t_0)})} \\ &\times \exp\left\{\frac{v_0 + v_T}{\eta^2}\left[\frac{\lambda(1 + e^{-\lambda(T-t_0)})}{(1 - e^{-\lambda(T-t_0)})} - \frac{\gamma(a)(1 + e^{-\gamma(a)(T-t_0)})}{(1 - e^{-\gamma(a)(T-t_0)})}\right]\right\} \\ &\times \frac{I_{\frac{1}{2}d-1}\left(\sqrt{v_0 v_T}\frac{4\gamma(a)e^{-\frac{1}{2}\gamma(a)(T-t_0)}}{\eta^2(1-e^{-\gamma(a)(T-t_0)})}\right)}{I_{\frac{1}{2}d-1}\left(\sqrt{v_0 v_T}\frac{4\lambda e^{-\frac{1}{2}\lambda(T-t_0)}}{\eta^2(1-e^{-\lambda(T-t_0)})}\right)},\end{aligned} \tag{2.11}$$

where $\gamma(a) = \sqrt{\lambda^2 - 2\eta^2\mathbf{i}a}$ and $d = 4\bar{v}\lambda/\eta^2$.

Proof. See [9]. □

In conclusion, the transition density for Bates model can be obtained following Eq.(2.9) with the transition density function $p(z_x, T - t_0|v_T, v_0)$ resulting from the discrete Fourier inverse transform w.r.t. ω of (2.10) and $p_v(v_T, T - t_0|v_0)$ given by Lemma 2.2.

Computing greeks. An important application of our integral representation formula (2.6) is the possibility of deriving closed-form expressions for the so called *greeks*, that are so important for hedging. In particular, the derivation of *delta* and *gamma* (respectively the first and second derivative of the option price with respect to the underlying asset price S) is straightforward. Other greeks, such as *vega*, can be more complicated. Nevertheless, in those cases one can easily resort to numerical differentiation by computing difference quotients from perturbed variable or parameter values. By way of example, we compute the analytical formula for the delta, that can be easily reiterated to compute the gamma as well. By the chain rule, we have $\Delta(S, v, t) = \dfrac{\partial V}{\partial S}(S, v, t) = \dfrac{1}{S}\dfrac{\partial u}{\partial x}(x, v, t)e^{-r(T-t)}$. From (2.6), Leibniz's rule for

differentiation under the integral sign gives

$$\begin{aligned}\frac{\partial u}{\partial x}(x,v,t) = &\int_{\Omega_x}\int_{\Omega_v}(e^y-E)^+\frac{\partial G}{\partial x}(y,w,T;x,v,t)dwdy+\\ &-\int_t^T\int_{\Omega_v}\frac{w}{2}\frac{\partial G}{\partial x}(\log(L),w,s;x,v,t)\frac{\partial u}{\partial y}(\log(L),w,s)dwds.\end{aligned} \tag{2.12}$$

Moreover,

$$\frac{\partial G}{\partial x}(y,w,T;x,v,t) = p_v(w,T-t|v)\frac{\partial p}{\partial x}(y-x,T-t|w,v)$$

and

$$\frac{\partial p}{\partial x}(y-x,T-t|w,v) = \frac{1}{2\pi}\int_{-\infty}^{+\infty}\hat{p}(\omega;v,w,T-t)\mathbf{i}\omega e^{-\mathbf{i}\omega(y-x)}d\omega.$$

Details on the computation of delta are discussed at the end of Section 4.

3. BEM numerical approximation. The Integral Representation formula (2.6) can be considered as a closed-form solution for barrier option pricing. However, the solution $u(x,v,t)$ is defined as a function of $\partial u/\partial y$ itself and, moreover, the Green function G is not available in explicit form and integration cannot be performed in exact form. Therefore, we have to resort to numerical approximation, through the so-called Boundary Element Method [11].
Consider the Integral Representation formula (2.6) and let $x \to \log(L)$. Taking into account the vanishing condition (2.5) on the option price at the log-barrier $\log(L)$, we obtain the Boundary Integral Equation (BIE)

$$\begin{aligned}0 = u(\log(L),v,t) :=&\int_{\log(L)}^{+\infty}\int_{\Omega_v}\max(e^y-E,0)G(y,w,T;\log(L),v,t)dw\,dy+\\ &-\int_t^T\int_{\Omega_v}\frac{w}{2}G(\log(L),w,\tau;\log(L),v,t)\frac{\partial u}{\partial y}(\log(L),w,\tau)dw\,d\tau\end{aligned} \tag{3.1}$$

whose sole unknown is the function $\frac{\partial u}{\partial y}(\log(L),w,\tau)$. Once solved numerically and obtained $\frac{\partial u}{\partial y}(\log(L),w,\tau)$, we can reconsider equation (2.6) to get the solution u wherever in the domain $\Omega_x \times \Omega_v$ at any instant in $[0,T]$.

We introduce a uniform decomposition $0 \equiv t_0 < t_1 < \ldots < t_{N_{\Delta t}} \equiv T$ of the time interval $[0,T]$ with time step $\Delta t = T/N_{\Delta t}$, $N_{\Delta t} \in \mathbb{Z}^+$ and we choose temporally piecewise constant shape functions $\varphi_k(t) := H[t-t_{k-1}] - H[t-t_k]$, $k = 1,\ldots,N_{\Delta t}$, where $H[\cdot]$ denotes the Heaviside step function[3], for the approximation in time of the unknown $\frac{\partial V}{\partial y}(\log(L),w,\tau)$ in Eq.(3.1).
Figs. 1-3 show the fundamental solution obtained computing (2.9) by numerical inverse Fourier transform. As expected, we observe that: the fundamental solution rapidly goes to 0 along w-axis when $w \to +\infty$, it takes the form of a bell-shaped

[3]We define the Heaviside step function as:

$$H[t-t_k] = \begin{cases} 1 & \text{if } t > t_k \\ 0 & \text{if } t \le t_k \end{cases}.$$

distribution with mean $\overline{v}$ when τ increases along the τ-axis and it tends to a numerical Dirac Delta distribution centered in v when $\tau \to t = 0$.

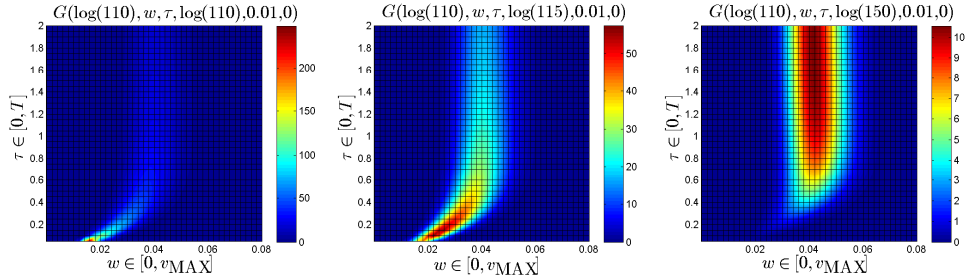

Fig. 1: Fundamental solution behavior with parameters of Example 2, varying the distance of y from the log-barrier $\log(L)$, when $v = 0.01$ is lower than $\overline{v} = 0.04$.

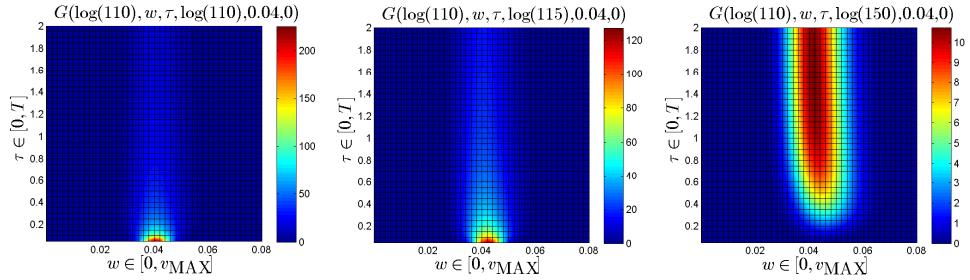

Fig. 2: Fundamental solution behavior with parameter of Example 1, varying the distance of y from the log-barrier $\log(L)$, when v is equal to $\overline{v} = 0.04$.

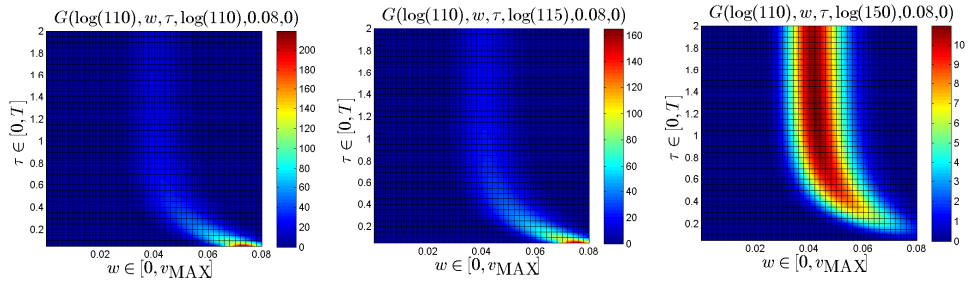

Fig. 3: Fundamental solution behavior with parameter of Example 1, varying the distance of y from the log-barrier $\log(L)$, when $v = 0.08$ is higher than $\overline{v} = 0.04$.

Moreover we know that as volatility approaches infinity, the price approaches a steady state ([22]). So, we can infer that there exists a value v_{MAX} such that integrals with kernel G involved in our discretization algorithm over interval $[v_{\mathrm{MAX}}, +\infty]$ are negligible (in our numerical examples we set $v_{\mathrm{MAX}} = 2 * \max(v, \overline{v})$); then we can

introduce a uniform decomposition of the truncated variance domain $[0, v_{\text{MAX}}]$ in $N_{\Delta v} \in \mathbb{Z}^+$ variance intervals of length $\Delta v := v_{\text{MAX}}/N_{\Delta v}$ and we can choose piecewise constant shape functions $\psi_h(t) := H[v - v_{h-1}] - H[v - v_h]$, $h = 1, \dots, N_{\Delta v}$ for the approximation in variance of the unknown function

$$\frac{\partial V}{\partial y}(\log(L), w, \tau) \approx q(w, \tau) := \sum_{h=1}^{N_{\Delta v}} \sum_{k=1}^{N_{\Delta t}} \alpha_h^{(k)} \psi_h(w) \varphi_k(\tau)\,. \tag{3.2}$$

Alternatively, we could resort to an infinite element approach as in [31], thus avoiding any domain truncation. After substituting $q(w, \tau)$, we evaluate equation (3.1) in the collocation points $(\overline{v}_i, \overline{t}_j)$ choosing, as usual when considering piecewise constant trial functions, barycenters of intervals $[v_{i-1}, v_i] \times [t_{j-1}, t_j]$

$$\overline{v}_i = \frac{v_i + v_{i-1}}{2},\ i = 1, \dots, N_{\Delta v} \qquad \overline{t}_j = \frac{t_j + t_{j-1}}{2},\ j = 1, \dots, N_{\Delta t}$$

and so obtaining a linear system whose unknowns are the coefficients of (3.2) collected in the vector $\alpha = \left(\alpha^{(k)}\big|_{k=1,\dots,N_{\Delta t}}\right) = \left((\alpha_h^{(k)}|_{h=1,\dots,N_{\Delta v}})\big|_{k=1,\dots,N_{\Delta t}}\right)$

$$\mathcal{A}\alpha = \mathcal{F} \tag{3.3}$$

with

$$\mathcal{A}_{ih}^{(jk)} = \int_{\overline{t}_j}^{T} \int_{\Omega_v} \frac{w}{2} G(\log(L), w, \tau; \log(L), \overline{v}_i, \overline{t}_j) \psi_h(w) \varphi_k(\tau) dw\, d\tau \tag{3.4}$$

and

$$\begin{aligned} \mathcal{F}_i^{(j)} &= \int_{\log(L)}^{+\infty} \int_{\Omega_v} \max(e^y - E, 0) G(y, w, T; \log(L), \overline{v}_i, \overline{t}_j) dw\, dy = \\ &= \int_{\log(L)}^{+\infty} \max(e^y - E, 0) \widetilde{G}(y, T; \log(L), \overline{v}_i, \overline{t}_j) dy, \end{aligned} \tag{3.5}$$

with $\widetilde{G}$ defined as in (2.7).
Note that, in system (3.3), $\mathcal{A}$ is a block-upper triangular Toeplitz matrix of dimension $N_{\Delta t}$ and its blocks have dimension $N_{\Delta v} \times N_{\Delta v}$

$$\begin{pmatrix} A^{(0)} & A^{(1)} & A^{(2)} & \cdots & A^{(N_{\Delta t}-1)} \\ 0 & A^{(0)} & A^{(1)} & \cdots & A^{(N_{\Delta t}-2)} \\ 0 & 0 & A^{(0)} & \ddots & \vdots \\ \vdots & \vdots & \ddots & \ddots & A^{(1)} \\ 0 & 0 & \cdots & 0 & A^{(0)} \end{pmatrix} \begin{pmatrix} \alpha^{(1)} \\ \alpha^{(2)} \\ \alpha^{(3)} \\ \vdots \\ \alpha^{(N_{\Delta t})} \end{pmatrix} = \begin{pmatrix} \mathcal{F}^{(1)} \\ \mathcal{F}^{(2)} \\ \mathcal{F}^{(3)} \\ \vdots \\ \mathcal{F}^{(N_{\Delta t})} \end{pmatrix} \tag{3.6}$$

as its elements depend on the difference $k - j = \ell$, $\ell = 0, \dots, N_{\Delta t} - 1$ and they reduce

to

(3.7)

$$
\begin{aligned}
&\mathcal{A}_{ih}^{(jk)} = \\
&= \int_{\max(\bar{t}_j, t_{k-1})}^{t_k} H[t_k - \max(\bar{t}_j, t_{k-1})] \int_{v_{h-1}}^{v_h} \frac{w}{2} G(\log(L), w, \tau; \log(L), \overline{v}_i, \bar{t}_j) dw\, d\tau = \\
&= \int_{\max(\bar{t}_j, t_{k-1})}^{t_k} H[t_k - \max(\bar{t}_j, t_{k-1})] \int_{v_{h-1}}^{v_h} \frac{w}{2} p_v(w, \tau - \bar{t}_j | \overline{v}_i) p(0, \tau - \bar{t}_j | w, \overline{v}_i) dw\, d\tau = \\
&= \int_{\max(\bar{t}_j, t_{k-1})}^{t_k} H[t_k - \max(\bar{t}_j, t_{k-1})] \int_{v_{h-1}}^{v_h} \frac{w}{4\pi} p_v(w, \tau - \bar{t}_j | \overline{v}_i) \int_{-\infty}^{+\infty} \widehat{p}(\omega; \overline{v}_i, w, \tau - \bar{t}_j) d\omega dw d\tau = \\
&= \int_{\frac{1}{2} - \frac{1}{2} H[\ell]}^{1} \int_{v_{h-1}}^{v_h} \frac{\Delta t}{4\pi} w\, p_v(w, \Delta t(\ell - \frac{1}{2} + s) | \overline{v}_i) \int_{-\infty}^{+\infty} \widehat{p}(\omega; \overline{v}_i, w, \Delta t(\ell - \frac{1}{2} + s)) d\omega dw ds = \\
&=: \mathcal{A}_{ih}^{(\ell)}
\end{aligned}
$$

as, with the change of variable $\tau = \Delta t(k + s - 1)$, we get $\tau - \bar{t}_j = \Delta t(k - j - \frac{1}{2} + s) = \Delta t(\ell - \frac{1}{2} + s)$.

For the numerical evaluation of (3.7) at last line we use:

- the adaptive quadrature rule of the Matlab function `Iquadgk` with an absolute tolerance 10^{-6} for the inner numerical Fourier inverse transform in ω evaluated at 0. We decide not to use the Fast Fourier Transform, despite its efficiency, in order to easily manage the accuracy and because we do not need to compute the inverse transform at a set of values but only at $y - x = \log(L) - \log(L) = 0$;
- the Gauss-Legendre quadrature rule for the integral in w over variance domain $[v_{h-1}, v_h]$. In order to save computation time and to keep accuracy, at each time τ, we use a different number of nodes (never higher than 64) depending of the fact that the integrand function may be peaked into the interval $[v_{h-1}, v_h]$ as suggested by Figs. 1-3;
- the Gauss-Legendre quadrature rule with 16 nodes for the outer integral in s over the time interval. To preserve accuracy, when we need to integrate the numerical Dirac Delta distribution (it happens when $\ell = 0$ and $\overline{v}_i \in [v_{h-1}, v_h]$), we have to concentrate the gaussian nodes towards the lower bound $\frac{1}{2} - \frac{1}{2} H[\ell] = \frac{1}{2}$ using for example the transformation for mild singularity suggested in [26][4].

Considering the evaluation of the rhs entries in (3.5), note that, from the numerical point of view, it is convenient to avoid the integration over the unbounded domain

[4] Consider the following integral

$$I = \int_a^b f(x)dx = \int_0^1 f\big((b-a)s + a\big)(b-a)ds$$

and then the transformation $\varphi : [0,1] \to [0,1]$ s.t. its derivatives $\varphi^{(i)}(0) = \varphi^{(j)}(1) = 0$ for $i = 1 \dots p-1$ and $j = 1 \dots q-1$:

$$\varphi(t) = \frac{(p+q-1)!}{(p-1)!(q-1)!} \int_0^t u^{p-1}(1-u)^{q-1} du\,.$$

We apply the Gauss-Legendre quadrature rule to the integral

$$I = \int_0^1 f\big((b-a)\varphi(t) + a\big)(b-a)\varphi'(t)dt\,,$$

it turns out that nodes move to the lower bound a if p increases and they move to the upper bound b if q increases.

$(\log(L), +\infty)$ and it is preferable to exploit the analytical solution of the plain vanilla European Call option problem in this way

(3.8)

$$\begin{aligned}
\mathcal{F}_i^{(j)} &= \int_{\log(L)}^{+\infty} \max(e^y - E, 0)\widetilde{G}(y, T; \log(L), \overline{v}_i, \overline{t}_j)dy \\
&= \int_{-\infty}^{+\infty} \max(e^y - E, 0)\widetilde{G}(y, T; \log(L), \overline{v}_i, \overline{t}_j)dy + \\
&\quad - \int_{-\infty}^{\log(L)} \max(e^y - E, 0)\widetilde{G}(y, T; \log(L), \overline{v}_i, \overline{t}_j)dy \\
&= \int_{-\infty}^{+\infty} \max(e^y - E, 0)\widetilde{G}(y, T; \log(L), \overline{v}_i, \overline{t}_j)dy + \\
&\quad - \int_{\log(E)}^{\log(L)} H[L - E](e^y - E)\widetilde{G}(y, T; \log(L), \overline{v}_i, \overline{t}_j)dy \\
&= EC(\log(L), \overline{v}_i, \overline{t}_j) - \int_{\log(E)}^{\log(L)} H[L - E](e^y - E)\widetilde{G}(y, T; \log(L), \overline{v}_i, \overline{t}_j)dy\,.
\end{aligned}$$

The first integral represents the solution (multiplied by $e^{r(T-t)}$) of an European Call option (EC) without barrier, that is the solution of Eq. (2.4) with the usual payoff condition $V(x, v, T) = \max(e^x - E, 0)$ and it can be analytically written as in [5]. It can be numerically computed, for example, as suggested in [10], but in this context we need it evaluated only at $x = \log(L), v = \overline{v}_i, t = \overline{t}_j$ so that it is convenient to simply compute the analytical solution written in [5] with standard quadrature rules:

(3.9)

$$EC(x, v, t) = e^{r(T-t)}\big(e^{-\delta(T-t)}e^x P_1(x, v, t) - Ee^{r(T-t)}P_2(x, v, t)\big) \quad \text{with}$$

$$P_i(x, v, t) = \frac{1}{2} + \frac{1}{\pi}\int_0^{+\infty} \mathrm{Re}\left(\frac{e^{-\mathbf{i}z\log(E)}}{\mathbf{i}z}e^{C_i(t,z)+D_i(t,z)v+\mathbf{i}zx+\mathrm{Jump}}\right)dz \quad i = 1, 2$$

$$C_i(t, z) = (r - \delta)z\mathbf{i}(T - t) + \frac{\lambda\overline{v}}{\eta^2}\left\{(\lambda + (i-2)\rho\eta - \rho\eta z\mathbf{i} + f_i)(T - t) - 2\log\left[\frac{1 - g_i e^{f_i(T-t)}}{1 - g_i}\right]\right\}$$

$$D_i(t, z) = \frac{\lambda + (i-2)\rho\eta - \rho\eta z\mathbf{i} + f_i}{\eta^2}\left[\frac{1 - e^{f_i(T-t)}}{1 - g_i e^{f_i(T-t)}}\right]$$

$$g_i = \frac{\lambda + (i-2)\rho\eta - \rho\eta z\mathbf{i} + f_i}{\lambda + (i-2)\rho\eta - \rho\eta z\mathbf{i} - f_i}$$

$$f_i = \sqrt{(\rho\eta z\mathbf{i} - \lambda - (i-2)\rho\eta)^2 - \eta^2\left(z\mathbf{i}(-1)^{i+1} - z^2\right)}$$

$$\mathrm{Jump} = -\mathbf{i}\xi\overline{k}z(T - t) + \xi(1 + \overline{k})^{2-i}(T - t)\left[(1 + \overline{k})^{\mathbf{i}z}e^{\left((-1)^{i-1}+\mathbf{i}z\right)\mathbf{i}z\sigma_j^2/2} - 1\right] \quad .$$

The improper integral in the P_i expression is easy to compute numerically because the integrand function is smooth and it decays rapidly, therefore also in this case we used the Matlab function `quadgk` that implements an adaptive quadrature rule over an infinite interval.

The second integral in (3.8) is computed by a Gaussian quadrature rules with 32 nodes.

Once all the elements of linear system (3.6) have been evaluated, due to the particular structure (3.6) of matrix $\mathcal{A}$, the approximate solution $q(w, \tau)$ of the BIE (3.1), expressed by the vector of coefficients α in (3.2), can be obtained by block-backward

substitution: the only matrix to be inverted is the diagonal block $\mathcal{A}^{(0)}$, the others update at every time step the right-hand side.
Then, one more step is necessary in order to get the undiscounted price of barrier option $u(x,v,t)$ in $\Omega_x \times \Omega_v$ for $t \in [0,T)$: we have to post-process α introducing it in Eq.(2.6) [5]

$$
\begin{aligned}
u(x,v,t) := & \int_{\log(L)}^{+\infty} \max(e^y - E, 0)\widetilde{G}(y,T;x,v,t)dy + \\
& - \sum_{h=1}^{N_{\Delta v}} \sum_{k=\text{floor}[\frac{t}{\Delta t}]+1}^{N_{\Delta t}} \alpha_h^{(k)} \int_{\max(t,t_{k-1})}^{t_k} \int_{v_{h-1}}^{v_h} \frac{w}{2} G(\log(L), w, \tau; x, v, t) dw\, d\tau \,.
\end{aligned} \tag{3.10}
$$

The first term on the right-hand side of (3.10) can be manipulated as the elements $F_i^{(j)}$ (look at (3.5) and (3.8))

$$
\int_{\log(L)}^{+\infty} \max(e^y - E, 0)\widetilde{G}(y,T;x,v,t)dy = EC(x,v,t) - \int_{\log(E)}^{\log(L)} (e^y - E)\widetilde{G}(y,T;x,v,t)dy \,. \tag{3.11}
$$

As usually we are interested in the option value at the time of evaluation $u(x,v,0)$, the second term on the right-hand side of (3.10) is

$$
\begin{aligned}
& - \sum_{h=1}^{N_{\Delta v}} \sum_{k=1}^{N_{\Delta t}} \alpha_h^{(k)} \int_{t_{k-1}}^{t_k} \int_{v_{h-1}}^{v_h} \frac{w}{2} G(\log(L), w, \tau; x, v, 0) dw\, d\tau = \\
& = - \sum_{h=1}^{N_{\Delta v}} \sum_{k=1}^{N_{\Delta t}} \alpha_h^{(k)} \int_{t_{k-1}}^{t_k} \int_{v_{h-1}}^{v_h} \frac{w}{2} p_v(w,\tau|v) p(\log(L) - x, \tau | w, v) dw\, d\tau = \\
& = - \sum_{h=1}^{N_{\Delta v}} \sum_{k=1}^{N_{\Delta t}} \alpha_h^{(k)} \int_{t_{k-1}}^{t_k} \int_{v_{h-1}}^{v_h} \frac{w}{4\pi} p_v(w,\tau|v) \int_{-\infty}^{+\infty} \widehat{p}(\omega; v, w, \tau) e^{-\mathbf{i}\omega(\log(L)-x)} d\omega dw\, d\tau = \\
& = - \sum_{h=1}^{N_{\Delta v}} \sum_{k=1}^{N_{\Delta t}} \alpha_h^{(k)} \int_0^1 \int_{v_{h-1}}^{v_h} \frac{\Delta t}{4\pi} w\, p_v(w, \Delta t(k-1+s)|v) \cdot \\
& \qquad \cdot \int_{-\infty}^{+\infty} \frac{\widehat{p}(\omega; v, w, \Delta t(k-1+s))}{e^{\mathbf{i}\omega(\log(L)-x)}} d\omega dw\, ds
\end{aligned} \tag{3.12}
$$

and it can be computed as done with the linear system entries.
Finally to get the price of the contingent claim we applied the relation $V(S,v,0) = u(x,v,0)e^{-rT}$.
The above described techniques for the computation of both linear system entries and postprocessing are only a possible way to implement our BEM procedure. They have been performed in order to reach a precision of, at least, 10^{-5} w.r.t. the values obtained through the Matlab functions `dblquad` and `triplequad`, but significantly reducing computational time. However, we think that computation times could be lowered, though preserving accuracy.

[5] floor[·]:=function that rounds its argument to the nearest integers towards minus infinity.

4. Numerical results. We show the performance of the proposed method by means of two examples: the first in the Heston framework and the second under the more general Bates model. A theoretical analysis of the convergence of the numerical method developed in Section 3 appears to be a difficult task, due to the different kinds of approximations involved (the BEM integral formulation, the Fourier inverse transform, the numerical approximation of the integrals). Hence the accuracy of the method proposed is tested by numerical simulation.
In order to show the efficiency of our semi closed-form pricing formula with respect to other approximation methods, we implement a Monte Carlo (MC) simulation. The implementation of MC method is complicated by two aspects: first, the barrier option is path-dependent; second, the underlying process may perform jumps. This makes more difficult to compute functionals like $\inf_{t\leq T} S_t$, which depend on the entire trajectory and not only on its values at discrete times. To overcome this problem, one can exploit the independence of the continuous and jump parts. Therefore, in the intervals between jumps the process is continuous and increments of the diffusion can be approximated with an Euler scheme. Moreover, the diffusion law on sufficiently small intervals, conditionally on the values at its ends, may be approximated by a Brownian bridge and the probability that a trajectory does not breach the barrier between jumps can be computed as in [20] (p. 368). These probabilities can be used to weight the final payoff at maturity. This approach is known as *conditional Monte Carlo* and may reduce the bias and variance of a naive approach.
All the numerical simulations have been performed using a laptop computer (CPU Intel i5, 4Gb RAM).

Example I: European down-and-out call option in the Heston framework. In this example we used the parameter values that are suggested in [25] but setting $\xi = \mu_j = \sigma_j = 0$ and so naturally reducing to Heston framework:

(4.1)

Heston parameters		*Jumps parameters*	
speed of mean reversion	$\lambda = 4$;	intensity	$\xi = 0$;
long run mean level of variance	$\overline{v} = 0.04$;	jumps expectation	$\mu_j = 0$;
correlation	$\rho = -0.5$;	jumps variance	$\sigma_j = 0$;
volatility of volatility	$\eta = 0.1$;	*Evaluation Point*	
free risk interest rate	$r = 0.05$;		
dividend yield	$\delta = 0.02$;	current time	$t = 0$;
strike price	$E = 100$;	current variance	$v = 0.01$;
down barrier value	$L = 110$;	current price	S.

The expiry of the option is at $T = 1$. Therefore, the chosen domain of definition of the pricing problem is the time interval $[0, T] = [0, 1]$, the variance interval $[0, v_{\text{MAX}}] \approx \Omega_v$ with $v_{\text{MAX}} = 0.08$ and the price interval $\Omega_S = (L, +\infty)$.
Firstly, we investigate stability and convergence of BEM numerical approximation varying discretization parameters in time $N_{\Delta t}$ and in variance $N_{\Delta v}$: to do this, we evaluate the option price $V(S, v, t)$ at $t = 0$ near the down barrier value at $S = 115$ and far from it at $S = 150$. Looking at Tables 1-2, we can observe the gradual stabilization of option prices separately and jointly refining both in time and in variance space.

S =115	$N_{\Delta v}$ =3	$N_{\Delta v}$ =6	$N_{\Delta v}$ =9	$N_{\Delta v}$ =12	$N_{\Delta v}$ =15
$N_{\Delta t}$ =3	8.3170E+00	8.3167E+00	8.3127E+00	8.3113E+00	8.3107E+00
$N_{\Delta t}$ =6	8.3356E+00	8.3244E+00	8.3212E+00	8.3200E+00	8.3195E+00
$N_{\Delta t}$ =9	8.3354E+00	8.3259E+00	8.3227E+00	8.3215E+00	8.3210E+00
$N_{\Delta t}$ =12	8.3353E+00	8.3265E+00	8.3232E+00	8.3220E+00	8.3215E+00
$N_{\Delta t}$ =15	8.3356E+00	8.3267E+00	8.3235E+00	8.3223E+00	8.3218E+00

Table 1: Table of option values V(115,0.01,0) as a function of the discretization parameters.

S =150	$N_{\Delta v}$ =3	$N_{\Delta v}$ =6	$N_{\Delta v}$ =9	$N_{\Delta v}$ =12	$N_{\Delta v}$ =15
$N_{\Delta t}$ =3	5.1022E+01	5.1032E+01	5.1033E+01	5.1033E+01	5.1033E+01
$N_{\Delta t}$ =6	5.1015E+01	5.1025E+01	5.1026E+01	5.1026E+01	5.1026E+01
$N_{\Delta t}$ =9	5.1013E+01	5.1023E+01	5.1024E+01	5.1024E+01	5.1024E+01
$N_{\Delta t}$ =12	5.1012E+01	5.1022E+01	5.1023E+01	5.1023E+01	5.1023E+01
$N_{\Delta t}$ =15	5.1012E+01	5.1022E+01	5.1022E+01	5.1023E+01	5.1023E+01

Table 2: Table of option values V(150,0.01,0) as a function of the discretization parameters.

To simplify the comprehension of the two tables, Figure 4 shows a graphical evidence of the reduction of the relative error for increasing $N_{\Delta t}$ and $N_{\Delta v}$. The numerical solution with the finest discretization is used as the benchmark solution. The left panels refer to the case $S = 115$ and show the behavior of the error of the prices contained in the columns of Table 1 as a function of $N_{\Delta t}$ (at the top) and of the error of the prices contained in the rows of Table 1 as a function of $N_{\Delta v}$ (at the bottom). Columns and rows from 1 to 5 are denoted by different colors with the following order: blue, green, red, light blue, magenta. The right panels refer to the case $S = 150$ and show the behavior of the error of the prices contained in the columns and rows of Table 2 using the same layout. All the graphs show very similar behaviors. It is evident that fixing either $N_{\Delta t} = 3, 6, 9$ or $N_{\Delta v} = 3, 6, 9$ (blue, green and red lines), while giving sensible results, hinders the convergence. On the contrary, fixing larger values of one of the discretization parameters, say $N_{\Delta t} = 12, 15$ allows for very fast convergence for increasing $N_{\Delta v}$ (light blue and magenta lines). The same happens when we exchange roles of $N_{\Delta t}$ and $N_{\Delta v}$.

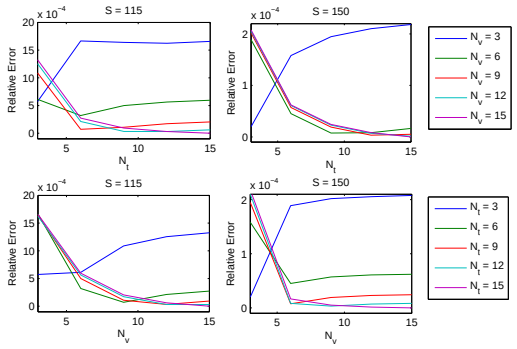

Fig. 4: Heston model. Relative pricing errors for increasing $N_{\Delta t}$ and $N_{\Delta v}$.

The convergence rate of BEM appears to be very fast in both time and variance. The rate of decay of the error benefits from the high order of regularity of the solution in the interior of the integration domain and we can observe that the error decays

exponentially with respect to both $N_{\Delta t}$ and $N_{\Delta v}$. Exponential decay of the error can be pointed out by plotting errors on a semilogarithmic scale, since the logarithm of the error should be approximately linear. Figure 5 shows the reduction of the absolute errors on a semilogarithmic scale for increasing $N_{\Delta t}$ and $N_{\Delta v}$. As expected, the spectral convergence is clearly achieved both at $N_{\Delta t} = 15$ w.r.t. the variance dimension and at $N_{\Delta v} = 15$ in time dimension, as denoted by the approximately linear dependence of the magenta lines. The circles correspond to the errors on the diagonal of Tables 1 and 2, i.e. when $N_{\Delta t}$ and $N_{\Delta v}$ are increased simultaneously. Also along the diagonals the convergence can be considered exponential.

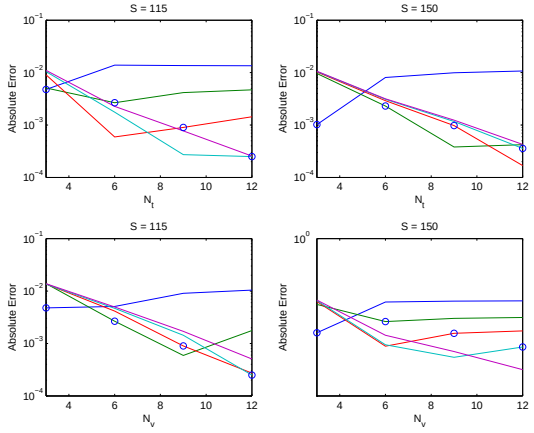

Fig. 5: Heston model. Absolute pricing errors for increasing $N_{\Delta t}$ and $N_{\Delta v}$ on a base 10 logarithmic scale for the y-axis and a linear scale for the x-axis.

Moreover, we checked also if the number of Gauss quadrature nodes and if the truncation value v_{MAX} of the variance domain have been correctly chosen. Therefore, we have repeated simulations doubling the number of quadrature nodes (Table 3) and increasing the value v_{MAX} (Table 4). Table 3 shows the absolute errors achieved w.r.t. the values in Tables 1-2. We note that the improvement in results is not significant in terms of the target accuracy.

$N_{\Delta t} = N_{\Delta v}$	3	6	9	12	15
S =115	2.9E-05	1.6E-06	2.4E-07	5.3E-08	2.0E-07
S =150	8.5E-11	2.3E-09	4.9E-09	9.7E-08	5.2E-08

Table 3: Difference between option values in Tables 1-2 and option values obtained with same discretization parameters but doubling the number of Gauss quadrature nodes.

The same happens if we enlarge the variance interval increasing v_{MAX} as in Table 4.

$N_{\Delta t}$	3	6	9	12	15
S =115	1.4E-06	1.7E-07	2.8E-07	3.2E-07	3.3E-07
S =150	1.2E-06	4.0E-06	5.0E-06	5.1E-06	5.1E-06

Table 4: Difference between option values in Tables 1-2 and option values obtained with same discretization parameters but enlarging the variance space, i.e. setting $v_{\text{MAX}} = \frac{4}{3}\,0.08$ (accordingly $N_{\Delta v} = \frac{4}{3}N_{\Delta t}$).

From the point of view of time employed in computation, in Table 5 we can see, on the left, computation times for $S = 115$ and, on the right, those for $S = 150$. The difference is not due to the fact that we are "near" or "far" from the barrier, but to the fact that the left panel shows the time for both pre and post-processing while the right panel shows only post-processing time. This represents an operative advantage of BEM: if we need to compute the option price for a new asset value (in this case for $S = 150$) we do not need to repeat the whole procedure but we can implement only the post-processing in Eq. 3.10 with a great computational saving.

BEM, $S = 115$
pre and post-processing

$N_{\Delta t} = N_{\Delta v}$	times
3	1.5E+02 s.
6	7.5E+02 s.
9	3.4E+03 s.
12	3.7E+03 s.
15	6.2E+03 s.

BEM, $S = 150$
post-processing

$N_{\Delta t} = N_{\Delta v}$	times
3	3.8E+01 s.
6	1.4E+02 s.
9	3.1E+02 s.
12	3.9E+02 s.
15	6.1E+02 s.

Table 5: Computation times of BEM method.

When comparing with MC method, the BEM method seems to be more reliable from the point of view of accuracy and also more efficient. In Tables 6-9, N represents the number of random samples and M the number of time steps in Euler time discretization in MC.

S=115

M	$N = 10^4$	95% conf. int.	$N = 10^6$	95% conf. int.	$N = 10^8$	95% conf. int.
100	8.3410E+00	[8.01,8.67]	8.3198E+00	[8.29,8.35]	8.3353E+00	[8.33,8.34]
200	8.1367E+00	[7.81,8.47]	8.3356E+00	[8.30,8.37]	8.3291E+00	[8.33,8.33]
400	8.2543E+00	[7.92,8.59]	8.3295E+00	[8.30,8.36]	8.3254E+00	[8.32,8.33]
800	8.3002E+00	[7.96,8.64]	8.3256E+00	[8.29,8.36]	8.3261E+00	[8.32,8.33]
1600	8.1777E+00	[7.85,8.51]	8.3229E+00	[8.29,8.36]	8.3231E+00	[8.32,8.33]

Table 6: Option value approximations of $V(115, 0.01, 0)$ and 95% confidence intervals obtained using Monte Carlo method, with respect to the number of samples N and the number of time steps M.

Monte Carlo, $S = 115$

M	$N = 10^4$	$N = 10^6$	$N = 10^8$
100	4.8E-01 s.	4.4E+01 s.	4.5E+03 s.
200	7.6E-01 s.	6.5E+01 s.	5.1E+03 s.
400	1.2E+00 s.	1.1E+02 s.	1.7E+04 s.
800	2.0E+00 s.	1.9E+02 s.	2.1E+04 s.
1600	3.6E+00 s.	3.5E+02 s.	4.2E+04 s.

Table 7: Computation times of Monte Carlo method for $S = 115$.

S=150

M	$N = 10^4$	95% conf. int.	$N = 10^6$	95% conf. int.	$N = 10^8$	95% conf. int.
100	5.1282E+01	[50.74,51.82]	5.1016E+01	[50.96,51.07]	5.1030E+01	[51.02,51.04]
200	5.1069E+01	[50.53,51.61]	5.1031E+01	[50.98,51.09]	5.1028E+01	[51.02,51.03]
400	5.1228E+01	[50.68,51.77]	5.1043E+01	[50.99,51.10]	5.1026E+01	[51.02,51.03]
800	5.1274E+01	[50.73,51.82]	5.1049E+01	[50.99,51.10]	5.1027E+01	[51.02,51.03]
1600	5.1357E+01	[50.82,51.90]	5.1052E+01	[51.00,51.11]	5.1029E+01	[51.02,51.03]

Table 8: Option value approximations of $V(150, 0.01, 0)$ and 95% confidence intervals obtained using Monte Carlo method, with respect to the number of samples N and the number of time steps M.

Monte Carlo, $S = 150$

M	$N = 10^4$	$N = 10^6$	$N = 10^8$
100	6.4E-01 s.	6.4E+01 s.	6.3E+03 s.
200	9.8E-01 s.	9.6E+01 s.	9.3E+03 s.
400	1.6E+00 s.	1.6E+02 s.	1.6E+04 s.
800	2.9E+00 s.	2.9E+02 s.	2.9E+04 s.
1600	5.5E+00 s.	5.4E+02 s.	5.2E+04 s.

Table 9: Computation times of Monte Carlo Method for $S = 150$.

Due to the fact that Monte Carlo method has rate of convergence of order $\sqrt{N}$, as expected, multiplying by 100 the number of samples, you can see in Tables 6 and 8 that we get about one more digit of accuracy in option price; however, the computational times become 100 times larger as shown in Tables 7 and 9. In relation to the number M of time steps of discretization, we cannot appreciate any sensible improvement in convergence. This may be due to the computation of the conditional expectation, that reduces the bias due to the time discretization. Moreover, we note that far from the barrier, i.e. at $S = 150$, the MC computational time seems to be slightly higher because the underlying asset rarely hits the barrier and we must therefore compute every survival probability for M steps, thus requiring greater computational effort per path.
Making the comparison, with $N = 10^8$ and a computation time of about 10^3 seconds, with MC method we are not able to reach an accuracy on the option price of order 10^{-2}, both at $S = 115$ and at $S = 150$. On the contrary, this level of accuracy can be easily reached with BEM. In particular, BEM seems to be even more accurate at $S = 150$, because "far" from the barrier, integrals are easily better evaluated. If we can settle of a smaller accuracy, say of order 10^{-1}, MC method appears to be more efficient: about 10^{-1} seconds of computation time with respect to 10^2 seconds for BEM in the best case, but we have to note that computation time in BEM can be reduced setting a lower accuracy threshold and a smaller number of nodes in the numerical evaluation of integrals.

Finally, since with BEM it is fast to make an evaluation of the option price as a function of the asset values, we can easily work out plots of the option price and, for instance, compare in Fig. 6 its behavior with the behavior of a call option without barrier: we observe that moving far from the barrier the two values tend to overlap, as expected.

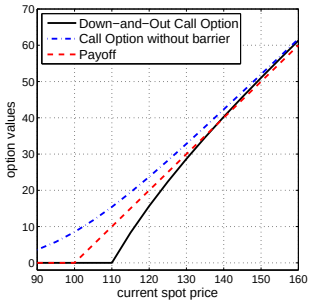

Fig. 6: In the Heston framework, value of a down-and-out call option compared with the value of a call option without barrier.

Example II: European down-and-out call option in the Bates framework. Consider the same parameters of Example I but introducing jumps:

(4.2)

Heston parameters		*Jumps parameters*	
speed of mean reversion	$\lambda = 4\,;$	intensity	$\xi = 4\,;$
long run mean level of variance	$\overline{v} = 0.04\,;$	jumps expectation	$\mu_j = -0.04\,;$
correlation	$\rho = -0.5\,;$	jumps variance	$\sigma_j = 0.06\,;$
volatility of volatility	$\eta = 0.1\,;$	*Evaluation Point*	
free risk interest rate	$r = 0.05\,;$		
dividend yield	$\delta = 0.02\,;$	current time	$t = 0\,;$
strike price	$E = 100\,;$	current variance	$v = 0.01\,;$
down barrier value	$L = 110\,;$	current price	$S\,.$

we can repeat the analysis above. The chosen domain of definition of the pricing problem is therefore the time interval $[0, T] = [0, 1]$, the variance interval $[0, v_{\text{MAX}}] \approx \Omega_v$ with $v_{\text{MAX}} = 0.08$ and the price interval $\Omega_S = (L, +\infty)$. In Tables 10 and 11 we list the results of our simulations, i.e. the option price at $t = 0$, $v = 0.01$ and $S = 115$ or $S = 150$, alternatively.

S =115	$N_{\Delta v}$ =3	$N_{\Delta v}$ =6	$N_{\Delta v}$ =9	$N_{\Delta v}$ =12	$N_{\Delta v}$ =15
$N_{\Delta t}$ =3	9.6050E+00	9.6156E+00	9.6022E+00	9.5975E+00	9.5956E+00
$N_{\Delta t}$ =6	9.6107E+00	9.6184E+00	9.6050E+00	9.6004E+00	9.5985E+00
$N_{\Delta t}$ =9	9.6113E+00	9.6191E+00	9.6057E+00	9.6010E+00	9.5992E+00
$N_{\Delta t}$ =12	9.6113E+00	9.6193E+00	9.6059E+00	9.6013E+00	9.5994E+00
$N_{\Delta t}$ =15	9.6114E+00	9.6194E+00	9.6060E+00	9.6013E+00	9.5995E+00

Table 10: Table of option values V(115,0.01,0) as a function of the discretization parameters.

S =150	$N_{\Delta v}$ =3	$N_{\Delta v}$ =6	$N_{\Delta v}$ =9	$N_{\Delta v}$ =12	$N_{\Delta v}$ =15
$N_{\Delta t}$ =3	5.0241E+01	5.0248E+01	5.0249E+01	5.0249E+01	5.0249E+01
$N_{\Delta t}$ =6	5.0234E+01	5.0241E+01	5.0242E+01	5.0242E+01	5.0242E+01
$N_{\Delta t}$ =9	5.0232E+01	5.0239E+01	5.0240E+01	5.0240E+01	5.0240E+01
$N_{\Delta t}$ =12	5.0231E+01	5.0238E+01	5.0239E+01	5.0239E+01	5.0239E+01
$N_{\Delta t}$ =15	5.0231E+01	5.0238E+01	5.0239E+01	5.0239E+01	5.0239E+01

Table 11: Table of option values V(150,0.01,0) as a function of the discretization parameters.

Again, to simplify the comprehension of the two tables, Figure 7 shows a graphical evidence of the reduction of the relative pricing errors for increasing $N_{\Delta t}$ and $N_{\Delta v}$, using the same layout of Figure 4. The comments are similar to the Heston case and convergence follows similar patterns as in Figure 4, with exponential rate only at $N_{\Delta t} = 12, 15$ and $N_{\Delta v} = 12, 15$.

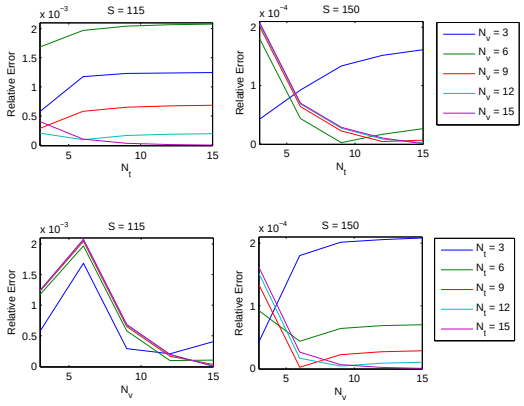

Fig. 7: Bates model. Relative pricing errors for increasing $N_{\Delta t}$ and $N_{\Delta v}$.

Figure 8 shows the reduction of the absolute errors on a semilogarithmic scale for increasing $N_{\Delta t}$ and $N_{\Delta v}$. Again, the spectral convergence is achieved at $N_{\Delta t} = 15$ and $N_{\Delta v} = 15$ respectively in space and time and on the diagonal of tables 10 and 11, i.e. when $N_{\Delta t}$ and $N_{\Delta v}$ are increased simultaneously.

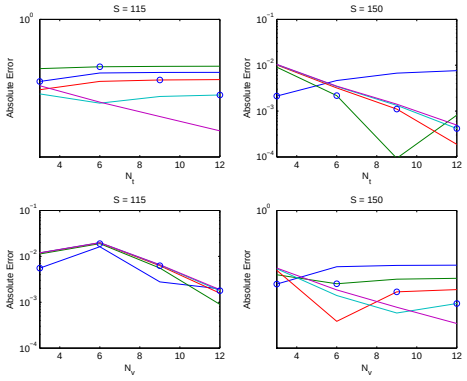

Fig. 8: Bates model. Absolute pricing errors for increasing $N_{\Delta t}$ and $N_{\Delta v}$ on a base 10 logarithmic scale for the y-axis and a linear scale for the x-axis.

The presence of jumps can be easily included in BEM technique and, looking at Tables 10, 11, it is clear that it influences the option values but not the stability and convergence of the method and not even the computational times, as evident in Table 12.

BEM, $S = 115$ pre and post-processing	
$N_{\Delta t} = N_{\Delta v}$	times
3	1.7E+02 s.
6	7.5E+02 s.
9	1.8E+03 s.
12	3.8E+03 s.
15	6.4E+03 s.

BEM, $S = 150$ post-processing	
$N_{\Delta t} = N_{\Delta v}$	times
3	4.4E+01 s.
6	1.5E+02 s.
9	2.6E+02 s.
12	4.6E+02 s.
15	6.6E+02 s.

Table 12: Computation times of BEM method.

This is not the case for MC method: in Table 13, we can observe that, multiplying by 10^2 the number of samples N, the improvement is lower than one digit of accuracy. Moreover, while in the Heston framework the discretization in time had not great impact, in Bates context it appears to be so significant as to introduce a bias: 95% confidence intervals in Table 13 are in some cases disjoint.
Computational memory and time request in Bates context is hundred times larger than in Heston framework (look at Tables 14, 16) so we are not able to increase discretization parameters M and N as we would need in order to achieve the desired accuracy. As a result, MC method would require very large values of M and N and hence much time to reach the same accuracy level of BEM. For example, for $V(150, 0.01, 0)$ the computation time required by BEM to get three significant digits correct is around 4.4E+01 s, while with MC it takes approximately 6.4E+03 s to get to the same level of accuracy. For $N = 10^8$ and $M = 400$ the performed Monte Carlo method is computationally too demanding: because of its computation memory request, it crashes during the simulation without reaching the end.

S=115

M	$N = 10^4$	95% conf. int.	$N = 10^6$	95% conf. int.	$N = 10^8$	95% conf. int.
100	9.4071E+00	[9.02,9.80]	9.6192E+00	[9.58,9.66]	9.6140E+00	[9.61,9.62]
200	9.4035E+00	[9.01,9.80]	9.5903E+00	[9.55,9.63]	9.5735E+00	[9.57,9.58]
400	9.7290E+00	[9.33,10.13]	9.5465E+00	[9.51,9.59]	/	/

Table 13: Option value approximations of $V(115, 0.01, 0)$ and 95% confidence intervals obtained using Monte Carlo method, as a function of the number of samples N and the number of time steps M.

Monte Carlo, $S = 115$

M	$N = 10^4$	$N = 10^6$	$N = 10^8$
100	2.4E+01 s.	2.3E+03 s.	3.1E+05 s.
200	4.8E+01 s.	4.6E+03 s.	6.1E+05 s.
400	9.6E+01 s.	9.2E+03 s.	/

Table 14: Computation times of Monte Carlo method for $S = 115$.

S=150

M	$N = 10^4$	95% conf. int.	$N = 10^6$	95% conf. int.	$N = 10^8$	95% conf. int.
100	5.0191E+01	[49.51,50.87]	5.0228E+01	[50.16,50.30]	5.0238E+01	[50.23,50.24]
200	4.9870E+01	[49.18,50.56]	5.0244E+01	[50.18,50.31]	5.0234E+01	[50.23,50.24]
400	4.9980E+01	[49.28,50.68]	5.0204E+01	[50.13,50.27]	/	/

Table 15: Option value approximations of $V(150, 0.01, 0)$ and 95% confidence intervals obtained using Monte Carlo method, as a function of the number of samples N and the number of time steps M.

Monte Carlo, $S = 150$

M	$N = 10^4$	$N = 10^6$	$N = 10^8$
100	3.25E+01 s.	3.23E+03 s.	3.08E+05s.
200	6.47E+01 s.	6.40E+03 s.	6.11E+05s.
400	1.28E+02 s.	1.22E+04 s.	/

Table 16: Computation times of BEM and Monte Carlo Method for $S = 150$.

As already observed, the post-processing formula (3.10) used in BEM method can be efficiently computed at every asset and variance values and at each time instant $t \in [0, T]$. This gives the opportunity to make a priori analysis of the investment or

to perform sensitivity analysis and compute greeks numerically. For instance, also for this last example, in Fig. 9 we can compare the behavior of the down-and-out call option to that of a European contract, as a function of the asset price S.

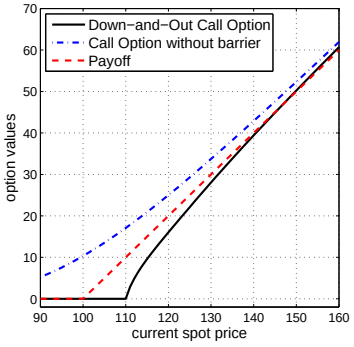

Fig. 9: In the Bates framework, value of a down-and-out call option compared with the value of a call option without barrier.

Moreover, in the post-processing phase, we can implement formula (2.12) and compute the delta of the option. In Table 17, we show evidence of the validity of formula (2.12) for computing the delta of the barrier option. The values of the delta at $S = 115$ and $S = 150$, obtained by (2.12) for $N_{\Delta t} = N_{\Delta v} = 6$, are compared to the ones computed from numerical differentiation. The quadrature formulas employed are the same used for the computation of the option value. The numerical delta is obtained by a second order difference quotient on the option prices obtained by post-processing (3.10) at $S - \Delta S$, S, $S + \Delta S$, for decreasing values of ΔS. We notice that at $S = 115$ the numerical delta rapidly converges to the (analytic) BEM value with a convergence ratio approximately equal to 4, which reveals the second order convergence of the difference quotients. At $S = 150$, the second order convergence of the numerical delta is affected by the fact that the difference quotients have been computed from option prices obtained with an error tolerance of 10^{-6} and hence numerical differentiation cannot improve this precision limit. In fact, at $S = 150$ the option value is almost linear (see Fig. 9) and the numerical delta rapidly approximates the exact value already for large values of ΔS.

	$S = 115$	BEM value = 0.013631583		$S = 150$	BEM value = 0.010614217	
ΔS	Num. delta	Abs. error	Conv. ratio	Num. delta	Abs. error	Conv. ratio
5	0.015996	2.3646E-03	-	0.010620	6.1343E-06	-
2.5	0.014041	4.0915E-04	(5.78)	0.010616	1.3077E-06	(4.69)
1.25	0.013721	8.9718E-05	(4.56)	0.010614	1.0139E-07	(12.90)
0.625	0.013653	2.1516E-05	(4.17)	0.010614	2.0017E-07	(0.507)
0.3125	0.013637	5.1465E-06	(4.18)	0.010614	2.7556E-07	(0.726)
0.15625	0.013633	1.0956E-06	(4.70)	0.010614	2.9441E-07	(0.936)

Table 17: Computation of the option delta. Comparison between BEM (analytic) procedure and numerical differentiation. The covergence ratio in parenthesis is the ratio between absolute errors on consecutive grids: $\text{error}_{\Delta S}/\text{error}_{\Delta S/2}$.

5. Conclusions. We have introduced and proved an analytical formula for pricing a down-and-out call option in the Heston/Bates framework. This formula can be

easily modified to get formulas for all kinds of barrier options in the Heston/Bates framework. We have also suggested a way to numerically compute the price and the most common greeks of the barrier option based on a Boundary Element Method approach.
One of the advantages of BEM over other PDE approaches is that the integral reformulation reduces by one the dimensionality of the partial differential problem, thus abating computation cost considerably. Furthermore, when multiple evaluations of the option contract are needed, one can implement only the post-processing formula (3.10) with a great computational saving and moreover the computation of derivative quantities, either analytic or numeric, is straightforward.
Being based on a closed-form integral formula for option pricing, it achieves spectral convergence in the interior of the integration domain. A rich convergence analysis and numerical evidence of greater accuracy and reduced computational cost in comparison with results achieved by Monte Carlo method highlight BEM as a valid and worthwhile alternative to traditional Monte Carlo approaches.

6. Acknowledgements. We wish to thank two anonymous referees for their helpful comments and remarks.

Appendix A. Boundary Element Formulation: Bates model. In this section we prove the integral representation formula (2.6) for the Bates model. For the reader's convenience, we first recall the notion of Green's solution from the classical theory of PIDEs.
We rewrite the PIDE (2.4) for a plain vanilla call option price V in the form

(A.1)
$$\begin{cases} \dfrac{\partial V}{\partial t}(x,v,t) + \mathcal{L}[V](x,v,t) + \mathcal{I}[V](x,v,t) - rV(x,v,t) = 0 & x \in \mathbb{R},\ v \in \Omega_v,\ t \in [0,T) \\ V(x,v,T) = \max(e^x - E, 0) & x \in \mathbb{R},\ v \in \Omega_v \end{cases}$$

where the operators $\mathcal{L}$ and $\mathcal{I}$ are defined as[6]

$$\mathcal{L}[V] = \frac{1}{2} v \frac{\partial^2 V}{\partial x^2} + \rho\eta v \frac{\partial^2 V}{\partial x \partial v} + \frac{1}{2}\eta^2 v \frac{\partial^2 V}{\partial v^2} + \left(r - \xi\bar{k} - \delta - \frac{1}{2} v \right) \frac{\partial V}{\partial x} - \lambda(v - \bar{v}) \frac{\partial V}{\partial v} \tag{A.2}$$

$$\begin{aligned} \mathcal{I}[V] &= \int_{-\infty}^{+\infty} [V(x+z,v,t) - V(x,v,t)] \nu(dz) \\ &= \xi\ \mathbb{E}[V(x+z,v,t) - V(x,v,t)] \\ &= \int_{-\infty}^{+\infty} [V(x+z,v,t) - V(x,v,t)] \xi \frac{1}{\sqrt{2\pi}\sigma_j} \exp\left(-\frac{(z-\mu_j)^2}{2\sigma_j^2} \right) dz \end{aligned} \tag{A.3}$$

and its solution is given by the fundamental pricing formula

$$V(x,v,t) = e^{-r(T-t)} \int_{-\infty}^{+\infty} \int_{\Omega_v} V(y,w,T) G(y,w,T;x,v,t)\, dw\, dy. \tag{A.4}$$

[6]For simplicity, we are assuming the market price of risk $\theta = 0$.

Observe that

$$u(x,v,t) := e^{r(T-t)}V(x,v,t) = \int_{-\infty}^{+\infty}\int_{\Omega_v} \max(e^y - E, 0)G(y,w,T;x,v,t)dw\,dy \tag{A.5}$$

is solution to the equation

$$\frac{\partial u}{\partial t}(x,v,t) + \mathcal{L}[u](x,v,t) + \mathcal{I}[u](x,v,t) = 0 \qquad x \in \mathbb{R},\, v \in \Omega_v,\, t \in [0,T) \tag{A.6}$$

with the same final condition as in (A.1). Here $G(x,y,v;w,t,\tau)$ is the *joint transition probability density function* (PDF), also known as *Green's function* or *fundamental solution* of the backward partial integro-differential problem.
It is well known ([18], [19]) that for each $(x,v,t) \in \mathbb{R}\times\mathbb{R}^+\times[0,T)$ the PDF $G(y,w,\tau;x,v,t)$, as a function of y,w,τ, solves the *forward Kolmogorov equation* (also known as the *Fokker-Planck equation*)

$$\begin{cases} -\dfrac{\partial G}{\partial \tau}(y,w,\tau;x,v,t) + \mathcal{L}^*[G](y,w,\tau;x,v,t) + \mathcal{I}^*[G](y,w,\tau;x,v,t) = 0 \\ \qquad\qquad\qquad\qquad\qquad\qquad\qquad\qquad\qquad\qquad y \in \mathbb{R},\, w \in \Omega_v,\, t < \tau \\ G(y,w,t;x,v,t) = \delta(x,y)\delta(v,w) \qquad\qquad\qquad\qquad\qquad\qquad y \in \mathbb{R},\, w \in \Omega_v \end{cases} \tag{A.7}$$

where $\delta(\cdot,\cdot)$ represents the Dirac distribution[7] and $\mathcal{L}^*$, $\mathcal{I}^*$ are the *adjoint operators* of $\mathcal{L}$ and $\mathcal{I}$ respectively[8], defined by

$$\begin{aligned} \mathcal{L}^*[\psi] = {} & \frac{1}{2}w\frac{\partial^2\psi}{\partial y^2} + \rho\eta w\frac{\partial^2\psi}{\partial y\partial w} + \frac{1}{2}\eta^2 w\frac{\partial^2\psi}{\partial w^2} - \left(r - \xi\bar{k} - \delta - \frac{1}{2}w\right)\frac{\partial\psi}{\partial y} + \lambda(w-\bar{v})\frac{\partial\psi}{\partial w} + \\ & + \rho\eta\frac{\partial\psi}{\partial y} + \eta^2\frac{\partial\psi}{\partial w} + \lambda(\cdot) = \\ & = \frac{1}{2}\frac{\partial^2\big(w\psi\big)}{\partial y^2} + \rho\eta\frac{\partial^2\big(w\psi\big)}{\partial y\partial w} + \frac{1}{2}\eta^2\frac{\partial^2\big(w\psi\big)}{\partial w^2} - \frac{\partial\big((r - \xi\bar{k} - \delta - \frac{1}{2}w)\psi\big)}{\partial y} + \\ & + \frac{\partial\big(\lambda(w-\bar{v})\psi\big)}{\partial w}, \end{aligned}$$

$$\mathcal{I}^*[\psi] = \int_{-\infty}^{+\infty}[\psi(y-z,w,\tau) - \psi(y,w,\tau)]\nu(dz).$$

[7] The *Dirac's delta distribution* satisfies the property that $\int_{-\infty}^{+\infty}\delta(y,x)f(x)dx = f(y)$, $\forall f \in \mathcal{C}_0^\infty(\mathbb{R})$.

[8] The adjoint operator is defined by the condition $< \mathcal{I}(\varphi), \psi > = < \varphi, \mathcal{I}^*(\psi) >$. In fact, for any smooth functions $\psi(y)$ and $\varphi(y)$ we have

$$\int_{-\infty}^{+\infty}\mathcal{I}[\varphi](y)\psi(y)dy = \int_{-\infty}^{+\infty}\varphi(y)\mathcal{I}^*[\psi](y)dy,$$

namely

$$\int_{-\infty}^{+\infty}\xi\mathbb{E}[\varphi(y+z) - \varphi(y)]\psi(y)dy = \int_{-\infty}^{+\infty}\xi\varphi(y)\mathbb{E}[\psi(y-z) - \psi(y)]dy,$$

since $\int_{-\infty}^{+\infty}\mathbb{E}[\varphi(y+z)]\psi(y)dy = \int_{-\infty}^{+\infty}\varphi(y)\mathbb{E}[\psi(y-z)]dy$.

When we consider a down-and-out Barrier Call Option, defining L the lower barrier for the asset S and setting $x = \log(S)$, the domain of investigation for the undiscounted price of the option $u(x, v, t)$ is $\Omega \times [0, T]$ where $\Omega = \Omega_x \times \Omega_v = [\log(L), +\infty) \times [0, +\infty)$. However, as remarked by [13] at p. 390, the nonlocal nature of the integral operator in (2.4) requires to specify the behavior of the solution not only *at* the barrier $x = \log L$, but also *beyond* the barrier for $x < \log L$. To compute the integral implicit in the expected value of the integral term, we need the function $u(\cdot, v, t)$ to be defined for all the values which the process can jump to from x by any jump in the support of the Lévy measure ν, i.e. everywhere in $\mathbb{R}$, and the natural extension is to set the option value below the barrier equal to zero. Therefore, the partial integro-differential formulation for a down-and-out call option is

$$\begin{cases} \dfrac{\partial u}{\partial t}(x, v, t) + \mathcal{L}[u](x, v, t) + \mathcal{I}[u](x, v, t) = 0 & x \in (\log(L), +\infty),\ v \in \Omega_v,\ t \in [0, T) \\ u(x, v, T) = \max(e^x - E, 0) & x \in (\log(L), +\infty),\ v \in \Omega_v \\ u(x, v, t) = 0 & x \in (-\infty, \log(L)],\ v \in \Omega_v,\ t \in [0, T) \end{cases}$$

and the Integral Representation (A.5) in the new domain $\Omega = \Omega_x \times \Omega_v$ has one more term

$$\begin{aligned} u(x, v, t) := & \int_{\log(L)}^{+\infty} \int_{\Omega_v} \max(e^y - E, 0) G(y, w, T; x, v, t) dw\, dy + \\ & - \int_t^T \int_{\Omega_v} \frac{w}{2} G(\log(L), w, \tau; x, v, t) \frac{\partial u}{\partial y}(\log(L), w, \tau) dw\, d\tau, \end{aligned} \tag{A.8}$$

namely, we get the integral representation formula (2.6).

Proof of validity of the representation formula (A.8). For any given t, let us consider the Bates model equation for u

$$\frac{\partial u}{\partial \tau}(y, w, \tau) + \mathcal{L}[u](y, w, \tau) + \mathcal{I}[u](y, w, \tau) = 0 \qquad \forall \tau \in [t, T],\ y \in \Omega_x,\ w \in \Omega_v \tag{A.9}$$

with $\mathcal{L}$, $\mathcal{I}$ defined in (A.2) and (A.3), respectively. Multiply Eq. (A.9) by the fundamental solution $G(y, w, \tau; x, v, t)$, the PDE in (A.7) by $u(y, w, \tau)$, subtract them and integrate in time and space obtaining

(A.10)

$$\begin{aligned} & \int_t^T \int_{\Omega_v} \int_{\log(L)}^{+\infty} \left\{ G(y, w, \tau; x, v, t) \frac{\partial u}{\partial \tau}(y, w, \tau) + u(y, w, \tau) \frac{\partial G}{\partial \tau}(y, w, \tau; x, v, t) \right\} dy\, dw\, d\tau \\ & + \int_t^T \int_{\Omega_v} \int_{\log(L)}^{+\infty} \{ G(y, w, \tau; x, v, t) \mathcal{L}[u](y, w, \tau) - u(y, w, \tau) \mathcal{L}^*[G](y, w, \tau; x, v, t) \}\, dy\, dw\, d\tau \\ & + \int_t^T \int_{\Omega_v} \int_{-\infty}^{+\infty} \{ G(y, w, \tau; x, v, t) \mathcal{I}[u](y, w, \tau) - u(y, w, \tau) \mathcal{I}^*[G](y, w, \tau; x, v, t) \}\, dy\, dw\, d\tau \\ & = 0. \end{aligned}$$

The second integral in (A.10) verifies the following identity (look at the proof below)
(A.11)
$$\int_t^T \int_{\Omega_v} \int_{\log(L)}^{+\infty} \{G(y,w,\tau;x,v,t)\mathcal{L}[u](y,w,\tau) - u(y,w,\tau)\mathcal{L}^*[G](y,w,\tau;x,v,t)\}\, dy\, dw\, d\tau$$
$$= -\frac{1}{2}\int_t^T \int_{\Omega_v} wG(\log(L),w,\tau;x,v,t)\frac{\partial u}{\partial y}(\log(L),w,\tau)dw\, d\tau.$$

The third integral in (A.10) equals zero, by definition of adjoint operator. The first integral in (A.10) can be integrated by parts

$$\int_t^T \int_{\Omega_v} \int_{\log(L)}^{+\infty} \left\{ G(y,w,\tau;x,v,t)\frac{\partial u}{\partial \tau}(y,w,\tau) + u(y,w,\tau)\frac{\partial G}{\partial \tau}(y,w,\tau;x,v,t) \right\} dy\, dw\, d\tau$$
$$= \int_{\Omega_v} \int_{\log(L)}^{+\infty} \left\{ \int_t^T G(y,w,\tau;x,v,t)\frac{\partial u}{\partial \tau}(y,w,\tau)d\tau + u(y,w,\tau)G(y,w,\tau;x,v,t)\Big|_{\tau=t}^{\tau=T} \right.$$
$$\left. - \int_t^T \frac{\partial u}{\partial \tau}(y,w,\tau)G(y,w,\tau;x,v,t)\, d\tau \right\} dy\, dw$$
$$= \int_{\Omega_v} \int_{\log(L)}^{+\infty} u(y,w,T)G(y,w,T;x,v,t)dy\, dw - \int_{\Omega_v} \int_{\log(L)}^{+\infty} u(y,w,t)G(y,w,t;x,v,t)dy\, dw =$$

and taking into account the initial condition in (A.7), it remains

$$= \int_{\Omega_v} \int_{\log(L)}^{+\infty} u(y,w,T)G(y,w,T;x,v,t)dy\, dw - \int_{\Omega_v} \int_{\log(L)}^{+\infty} u(y,w,t)\delta(x,y)\delta(v,w)dy\, dw$$
$$= \int_{\Omega_v} \int_{\log(L)}^{+\infty} u(y,w,T)G(y,w,T;x,v,t)dy\, dw - u(x,v,t)\,.$$

The representation formula (A.8) follows immediately. □

Proof of the identity (A.11):
Let us rewrite the integrand in (A.11) in divergence form

$$G(y,w,\tau;x,v,t)\mathcal{L}[u](y,w,\tau) - u(y,w,\tau)\mathcal{L}^*[G](y,w,\tau;x,v,t) = \frac{\partial p_1}{\partial y} + \frac{\partial p_2}{\partial w}$$

with

$$p1 = \frac{1}{2}\left(Gw\frac{\partial u}{\partial y} - u\frac{\partial (Gw)}{\partial y}\right) + \left(r - \xi\bar{k} - \delta - \frac{w}{2}\right)Gu + \frac{\rho\eta}{2}\left(Gw\frac{\partial u}{\partial w} - u\frac{\partial (Gw)}{\partial w}\right)$$
$$p2 = \frac{\rho\eta}{2}\left(Gw\frac{\partial u}{\partial y} - u\frac{\partial (Gw)}{\partial y}\right) - \lambda(w-\bar{v})Gu + \frac{\eta^2}{2}\left(Gw\frac{\partial u}{\partial w} - u\frac{\partial (Gw)}{\partial w}\right)$$

and, applying the divergence theorem, we obtain
(A.12)
$$\int_t^T \int_{\Omega_v} \int_{\log(L)}^{+\infty} \{G(y,w,\tau;x,v,t)\mathcal{L}[u](y,w,\tau) - u(y,w,\tau)\mathcal{L}^*[G](y,w,\tau;x,v,t)\}\, dy\, dw\, d\tau$$
$$= \int_t^T \int_{\partial\Omega} (p_1,p_2)\cdot \mathbf{n}\, dy\, dw\, dt,$$

with $\mathbf{n}$ the outward normal vector on the boundary $\partial\Omega$, as specified in Fig. 10.

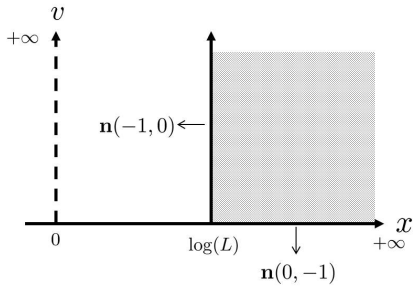

Fig. 10: Down-and-out barrier call option domain.

Taking into account the natural vanishing boundary conditions for the probability density function G as $y \to \pm\infty$ and $w \to 0$, $w \to +\infty$ and the barrier condition for u, the boundary integral reduces to[9]

$$\int_t^T \int_{\partial\Omega} (p_1, p_2) \cdot \mathbf{n}\, d\tau = -\int_t^T \int_{\{\log(L)\}\times\Omega_v} p_1\, dy\, dw\, d\tau$$

$$= -\int_t^T \int_{\Omega_v} \frac{1}{2}\left(Gw\frac{\partial u}{\partial y} - u\frac{\partial(Gw)}{\partial y}\right) + \left(r - \xi\bar{k} - \delta - \frac{w}{2}\right) Gu +$$

$$+\frac{\rho\eta}{2}\left(Gw\frac{\partial u}{\partial w} - u\frac{\partial(Gw)}{\partial w}\right)\Big|_{y=\log(L)} dw\, d\tau$$

$$= -\frac{1}{2}\int_t^T \int_{\Omega_v} \left(Gw\frac{\partial u}{\partial y} + \rho\eta Gw\frac{\partial u}{\partial w}\right)\Big|_{y=\log(L)} dw\, d\tau$$

$$= -\frac{1}{2}\int_t^T \int_{\Omega_v} wG(\log(L), w, \tau; x, v, t)\frac{\partial u}{\partial y}(\log(L), w, \tau) dw\, d\tau +$$

$$-\int_t^T \frac{\rho\eta}{2} wG(\log(L), w, \tau; x, v, t) u(\log(L), w, \tau) d\tau \Big|_{w=0}^{w\to+\infty} +$$

$$+\int_t^T \int_{\Omega_v} \frac{\rho\eta}{2}\left(G(\log(L), w, \tau; x, v, t) + w\frac{\partial G}{\partial w}(\log(L), w, \tau; x, v, t)\right) u(\log(L), w, \tau) dw\, d\tau$$

$$= -\frac{1}{2}\int_t^T \int_{\Omega_v} wG(\log(L), w, \tau; x, v, t)\frac{\partial u}{\partial y}(\log(L), w, \tau) dw\, d\tau. \quad \square$$

[9] In the case of a plain vanilla option, taking into account the vanishing boundary conditions for G on the boundary $\partial\Omega$ of the domain $\Omega = \Omega_v \times (-\infty, +\infty)$ as specified in Fig. 11, we get the so called *Green's Identity*

$$\int_t^T \int_{\Omega_v} \int_{-\infty}^{+\infty} \{G(y, w, \tau; x, v, t)\mathcal{L}[u](y, w, \tau) - u(y, w, \tau)\mathcal{L}^*[G](y, w, \tau; x, v, t)\}\, dy\, dw\, d\tau = 0$$

and, by substituting this into (A.10), we obtain the fundamental pricing formula (A.5).

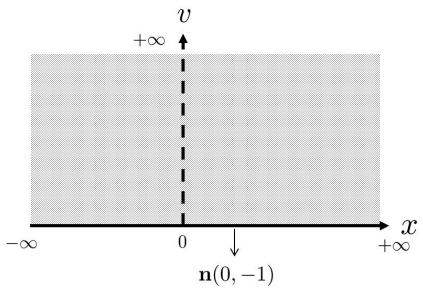

Fig. 11: Vanilla call option domain.

Appendix B. Joint transition probability density function. To prove Theorem 2.3, we need the following Lemma

LEMMA B.1. *The transition density for the Bates model can be written in terms of the change in the logarithmic stock price and the variance at maturity, given today's variance*

$$p(x_T, v_T, T; x_0, v_0, t_0) = p(z_x, v_T, T - t_0|v_0),$$

where $z_x = x_T - x_0$.

Proof. From the results in [16], [29] show that the two-dimensional conditional characteristic function for the Bates model can be written as

$$\phi_T(\omega_1, \omega_2; x_0, v_0, t_0) = \mathbb{E}_{t_0}[e^{\mathbf{i}\omega_1 x_T + \mathbf{i}\omega_2 v_T}] = e^{C(\omega_1,\omega_2,\tau)+J(\omega_1,\omega_2,\tau)+D(\omega_1,\omega_2,\tau)v_0+\mathbf{i}\omega_1 x_0},$$

where $\tau = T - t_0$ and C, J, D are suitable functions. Using the Gil-Pelaez inversion formula, we can obtain the joint transition density

$$\begin{aligned}
&p(x_T, v_T, T; x_0, v_0, t_0) = \\
&= \frac{1}{2\pi}\int_{-\infty}^{+\infty}\int_{-\infty}^{+\infty} Re(e^{C(\omega_1,\omega_2,\tau)+J(\omega_1,\omega_2,\tau)+D(\omega_1,\omega_2,\tau)v_0+\mathbf{i}\omega_1 x_0} e^{-\mathbf{i}\omega_1 x_T - \mathbf{i}\omega_2 v_T}) d\omega_1 d\omega_2 = \\
&= \frac{1}{2\pi}\int_{-\infty}^{+\infty}\int_{-\infty}^{+\infty} Re(e^{C(\omega_1,\omega_2,\tau)+J(\omega_1,\omega_2,\tau)+D(\omega_1,\omega_2,\tau)v_0-\mathbf{i}\omega_2 v_T - \mathbf{i}\omega_1 z_x}) d\omega_1 d\omega_2
\end{aligned}$$

which clearly depends on z_x, v_0, v_T and τ. The fact that the characteristic function is conditioned on time t_0 completes the proof. □

Proof. **of Theorem 2.3**. Equation (2.9) follows straightforwardly from Lemma B.1 and the relation

$$p(z_x, v_T, T - t_0|v_0) = p_v(v_T, T - t_0|v_0)p(z_x, T - t_0|v_T, v_0)\,.$$

It remains to compute the characteristic function $\hat{p}(\omega; v_0, v_T, T - t_0)$ of the logarithm of the stock given the initial variance v_0 and given the variance at maturity v_T. For this derivation, we follow [6] and we write the dynamics of the Bates model in a different manner

$$\begin{aligned}
dx_t &= \left(\mu - \frac{1}{2}v_t\right) + \rho\sqrt{v_t}dW_t^1 + \sqrt{1-\rho^2}\sqrt{v_t}dW_t^2 + j_N(t)dN(t) \\
dv_t &= -\lambda(v_t - \bar{v})dt + \eta\sqrt{v_t}dW_t^1,
\end{aligned} \tag{B.1}$$

where $\mu = r - \xi\bar{k}$ under the risk-neutral probability measure.
From (B.1) we get

$$\begin{aligned} x_T &= x_0 + \mu(T-t_0) - \frac{1}{2}\int_{t_0}^{T} v_s ds + \\ &+\rho\int_{t_0}^{T}\sqrt{v_s}dW_s^1 + \sqrt{1-\rho^2}\int_{t_0}^{T}\sqrt{v_s}dW_s^2 + \int_{t_0}^{T} j_N(s)dN(s), \end{aligned} \tag{B.2}$$

$$v_T = v_0 + \lambda\bar{v}(T-t_0) - \lambda\int_{t_0}^{T} v_s ds + \eta\int_{t_0}^{T}\sqrt{v_s}dW_s^1. \tag{B.3}$$

Rewriting equation (B.3) as

$$\eta\int_{t_0}^{T}\sqrt{v_s}dW_s^1 = v_T - v_0 - \lambda\bar{v}(T-t_0) + \lambda\int_{t_0}^{T} v_s ds$$

and substituting into (B.2), it gives

$$\begin{aligned} z_x &= x_T - x_0 = \mu(T-t_0) - \frac{1}{2}\int_{t_0}^{T} v_s ds \\ &+\frac{\rho}{\eta}\left(v_T - v_0 - \lambda\bar{v}(T-t_0) + \lambda\int_{t_0}^{T} v_s ds\right) + \sqrt{1-\rho^2}\int_{t_0}^{T}\sqrt{v_s}dW_s^2 + \int_{t_0}^{T} j_N(s)dN(s) \\ &= \mu(T-t_0) + \frac{\rho}{\eta}(v_T - v_0 - \lambda\bar{v}(T-t_0)) + \left(\frac{\lambda\rho}{\eta} - \frac{1}{2}\right)\int_{t_0}^{T} v_s ds \\ &+\sqrt{1-\rho^2}\int_{t_0}^{T}\sqrt{v_s}dW_s^2 + \int_{t_0}^{T} j_N(s)dN(s). \end{aligned}$$

Notice that $\int_{t_0}^{T}\sqrt{v_s}dW_s^2$ is normally distributed with zero expectation and variance equal to $\int_{t_0}^{T} v_s ds$ by Itô isometry. If we denote by Z a standard normal random variable, then the characteristic function $\hat{p}(\omega)$ conditional on v_0 and v_T reads

$$\begin{aligned} &\hat{p}(\omega; v_0, v_T, T-t_0) = \mathbb{E}_{t_0}\left[e^{\mathbf{i}\omega(x_T - x_0)}|v_T\right] \\ &= \mathbb{E}_{t_0}\left[\exp\left\{\mathbf{i}\omega\left[\mu(T-t_0) + \frac{\rho}{\eta}(v_T - v_0 - \lambda\bar{v}(T-t_0)) + \right.\right.\right. \\ &\left.\left.\left. + \left(\frac{\lambda\rho}{\eta} - \frac{1}{2}\right)\int_{t_0}^{T} v_s ds + \sqrt{1-\rho^2}\sqrt{\int_{t_0}^{T} v_s ds}Z + \int_{t_0}^{T} j_N(s)dN(s)\right]\right\}|v_T\right] \\ &= \exp\left\{\mathbf{i}\omega\left[\mu(T-t_0) + \frac{\rho}{\eta}(v_T - v_0 - \lambda\bar{v}(T-t_0))\right]\right\} \\ &\times\mathbb{E}_{t_0}\left[\exp\left\{\mathbf{i}\omega\left(\frac{\lambda\rho}{\eta} - \frac{1}{2}\right)\int_{t_0}^{T} v_s ds + \mathbf{i}\omega\sqrt{1-\rho^2}\sqrt{\int_{t_0}^{T} v_s ds}Z + \mathbf{i}\omega\int_{t_0}^{T} j_N(s)dN(s)\right\}|v_T\right]. \end{aligned}$$

Since jumps are homogeneous and independent of the continuous part, we get

$$\hat{p}(\omega; v_0, v_T, T-t_0) = \exp\left\{\mathbf{i}\omega\left[(r-\xi\bar{k})(T-t_0) + \frac{\rho}{\eta}(v_T - v_0 - \lambda\bar{v}(T-t_0))\right]\right\}$$
$$\times\mathbb{E}_{t_0}\left[\exp\left\{\mathbf{i}\omega\left(\frac{\lambda\rho}{\eta} - \frac{1}{2}\right)V + \mathbf{i}\omega\sqrt{1-\rho^2}\sqrt{V}Z\right\}|v_T\right]$$
$$\times\mathbb{E}_{t_0}\left[\exp\left\{\mathbf{i}\omega\int_{t_0}^{T} j_N(s)dN(s)\right\}|v_T\right],$$

where $V = \int_{t_0}^{T} v_s ds$. Using the tower property for expectations and taking into account the independence of the jump component from the variance process, we get

$$\hat{p}(\omega; v_0, v_T, T-t_0) = \exp\left\{\mathbf{i}\omega\left[(r-\xi\bar{k})(T-t_0) + \frac{\rho}{\eta}(v_T - v_0 - \lambda\bar{v}(T-t_0))\right]\right\}$$
$$\times\mathbb{E}_{t_0}\left[\mathbb{E}_{t_0}\left[\exp\left\{\mathbf{i}\omega\left(\frac{\lambda\rho}{\eta} - \frac{1}{2}\right)V + \mathbf{i}\omega\sqrt{1-\rho^2}\sqrt{V}Z\right\}\middle| v_T, V\right]\right]$$
$$\times\mathbb{E}_{t_0}\left[\exp\left\{\mathbf{i}\omega\int_{t_0}^{T} j_N(s)dN(s)\right\}\right] =$$
$$= \exp\left\{\mathbf{i}\omega\left[(r-\xi\bar{k})(T-t_0) + \frac{\rho}{\eta}(v_T - v_0 - \lambda\bar{v}(T-t_0))\right]\right\}$$
$$\times\mathbb{E}_{t_0}\left[\exp\left\{\mathbf{i}\omega\left(\frac{\lambda\rho}{\eta} - \frac{1}{2}\right)V - \frac{1}{2}\omega^2(1-\rho^2)V\right\}\middle| v_T\right]$$
$$\times\mathbb{E}_{t_0}\left[\exp\left\{\mathbf{i}\omega\int_{t_0}^{T} j_N(s)dN(s)\right\}\right] =$$
$$= \exp\left\{\mathbf{i}\omega\left[(r-\xi\bar{k})(T-t_0) + \frac{\rho}{\eta}(v_T - v_0 - \lambda\bar{v}(T-t_0))\right]\right\}$$
$$\times\mathbb{E}_{t_0}\left[\exp\left\{\mathbf{i}\left[\omega\left(\frac{\lambda\rho}{\eta} - \frac{1}{2}\right) + \frac{1}{2}\mathbf{i}\omega^2(1-\rho^2)\right]\int_{t_0}^{T} v_s ds\right\}|v_T\right]$$
$$\times\mathbb{E}_{t_0}\left[\exp\left\{\mathbf{i}\omega\int_{t_0}^{T} j_N(s)dN(s)\right\}\right] =$$
$$= \exp\left\{\mathbf{i}\omega\left[(r-\xi\bar{k})(T-t_0) + \frac{\rho}{\eta}(v_T - v_0 - \lambda\bar{v}(T-t_0))\right]\right\}$$
$$\times\Phi\left(\omega\left(\frac{\lambda\rho}{\eta} - \frac{1}{2}\right) + \frac{1}{2}\mathbf{i}\omega^2(1-\rho^2)\right)\ \phi_T^J(\omega),$$

where $\Phi(a)$ is defined by (2.11) and $\phi_T^J(\omega)$ by (2.2). This completes the proof. □

REFERENCES

[1] L.V. Ballestra A. Golbabai and D. Ahmadian, *A highly accurate finite element method to price discrete double barrier options*, Comput. Econ., 44 (2014).

[2] L.V. Ballestra and G. Pacelli, *Pricing double-barrier options using the boundary element method*, Working paper of Università Politecnica delle Marche, 33 (2009), pp. 1 – 42.

[3] ———, *A very fast and accurate boundary element method for options with moving barrier and time-dependent rebate*, Working paper of Università Politecnica delle Marche, 30 (2009), pp. 1 – 43.
[4] ———, *A boundary element method to price time-dependent double barrier options*, Applied Mathematics and Computation, 218 (2011), pp. 4192 – 4210.
[5] D.S. Bates, *Jumps and stochastic volatility: Exchange rate processes implicit in deutsche mark options*, The Review of Financial Studies, 9 (1996), pp. 69–107.
[6] F. Bervoets, *Model risk for exotic equity options*, msc Thesis Applied Mathematics, Delft University of Technology, 2006.
[7] F. Black and M. Scholes, *The pricing of options and corporate liabilities*, The Journal of Political Economy, 81 (1973), pp. 637–654.
[8] P.P. Boyle and S.H. Lau, *Bumping up against the barrier with the binomial method*, J. Derivatives, 2.
[9] M. Broadie and Ö. Kaya, *Exact simulation of stochastic volatility and other affine jump diffusion processes*, Oper. Res., 54 (2006), pp. 217–231.
[10] P. Carr, D.B. Madan, and R.H. Smith, *Option valuation using the fast fourier transform*, Journal of Computational Finance, 2 (1999), pp. 61–73.
[11] G. Chen and J. Zhou, *Boundary Element Methods*, Academic Press, 1992.
[12] A.H.-D. Cheng and D.T. Cheng, *Heritage and early history of the boundary element method*, Engineering Analysis with Boundary Elements, 29 (2005), pp. 268 – 302.
[13] R. Cont and P. Tankov, *Financial Modelling with Jump Processes*, Chapman & Hall/CRC, 2004.
[14] M. Costabel, In *Encyclopedia of Computational Mechanics*: Time-dependent problems with the boundary integral equation method, John Wiley and Sons, Ltd, 2004, pp. 1–28.
[15] J.C. Cox, J.E. Ingersoll Jr., and S.A. Ross, *A theory of the term structure of interest rates*, Econometrica, 53 (1985), pp. 385–407.
[16] D. Duffie, J. Pan, and K. Singleton, *Transform analysis and asset pricing for affine jump-diffusions.*, Econometrica, 68 (2000).
[17] W. Feller, *Two singular diffusion problems*, Ann. of Math. (2), 54 (1951), pp. 173–182.
[18] A. Friedman, *Stochastic Differential Equations and Applications*, Academic Press, 1975.
[19] M.G. Garroni and J.L. Menaldi, *Second order elliptic integro-differential problems*, Chapman & Hall/CRC, 2002.
[20] P. Glasserman, *Monte Carlo method in financial engineering*, Springer, 2004.
[21] C. Guardasoni and S. Sanfelici, *A boundary element approach to barrier option pricing in Black-Scholes framework*, International Journal of Computer Mathematics, forthcoming. DOI: 10.1080/00207160.2015.1020304 (2015).
[22] S.L. Heston, *A closed-form solution for options with stochastic volatility with applications to bond and currency options*, Review of Financial Studies, 6 (1993), pp. 327–343.
[23] I. Kitov and O. Kitov, *Unemployment and inflation in western europe: solution by the boundary element method*, Munich Personal RePEc Archive Paper, 14341 (2009), pp. 1 – 28.
[24] R. Merton, *Option pricing when underlying stock returns are discontinuous*, J. Fin. Economics, 3 (1976), pp. 125–144.
[25] E. Miglio and C. Sgarra, *A finite element discretization method for option pricing with the Bates model*, SēMA J., (2011), pp. 23–40.
[26] G. Monegato and L. Scuderi, *Numerical integration of functions with boundary singularities*, Journal of Computational and Applied Mathematics, 112 (1999), pp. 201–214.
[27] K.R. Vetzal P.A. Forsyth and R. Zvan, *Pde methods for pricing barrier options*, J. Econ. Dynam. Control, 24 (2000), pp. 1563–1590.
[28] P. Ritchken, *On pricing barrier options*, J. Derivatives, 3 (1991), pp. 19–28.
[29] M. Rockinger and M. Semenova, *Estimation of jump-diffusion processes via empirical characteristic functions.*, FAME Research Paper N. 150, (2005).
[30] L.C. Rogers and O. Zane, *Valuing moving barrier options*, J. Comput. Finance, 1 (1997), pp. 5–11.
[31] S. Sanfelici, *Galerkin infinite element approximation for pricing barrier options and options with discontinuous payoff*, Decis. Econ. Finance, 27 (2004), pp. 125–151.